Parameterization of OPLS–AA Force Field for the Conformational Analysis of Macrocyclic Polyketides

KALJU KAHN, THOMAS C. BRUICE

Department of Chemistry and Biochemistry, University of California, Santa Barbara,
Santa Barbara, California 93106

Abstract: The parameters for the OPLS–AA potential energy function have been extended to include some functional groups that are present in macrocyclic polyketides. Existing OPLS–AA torsional parameters for alkanes, alcohols, ethers, hemiacetals, esters, and ketoamides were improved based on MP2/aug-cc-pVTZ and MP2/aug-cc-pVDZ calculations. Nonbonded parameters for the sp^3 carbon and oxygen atoms were refined using Monte Carlo simulations of bulk liquids. The resulting force field predicts conformer energies and torsional barriers of alkanes, alcohols, ethers, and hemiacetals with an overall RMS deviation of 0.40 kcal/mol as compared to reference data. Densities of 19 bulk liquids are predicted with an average error of 1.1%, and heats of vaporization are reproduced within 2.4% of experimental values. The force field was used to perform conformational analysis of smaller analogs of the macrocyclic polyketide drug FK506. Structures that adopted low-energy conformations similar to that of bound FK506 were identified. The results show that a linker of four ketide units constitutes the shortest effector domain that allows binding of the ketide drugs to FKBP proteins. It is proposed that the exact chemical makeup of the effector domain has little influence on the conformational preference of tetraketides.

Introduction

Polyketides form a structurally diverse class of natural products whose biosynthesis takes place through the successive condensation of simple carboxylic acids.[1–3] Despite their widely varying size and structure, polyketides can be grouped into two superfamilies: the aromatic and the complex polyketides.[2] Some examples of aromatic polyketides include 6-methylsalicylic acid and tetracyclines, while erythromycins belong to the superfamily of complex polyketides. Many polyketides are pharmacologically active or possess useful agricultural properties. It is thought that the biological activity of complex polyketides is dependent on conformational preorganization, which directs functional groups in space and reduces the entropic penalty involved in binding.[4]

Some complex macrocyclic polyketides, such as FK506 (Chart 1) and its analogs, are promising neuroregenerative agents.[5,6] Their mechanism of action currently is poorly understood, but strong evidence suggests that interaction of a polyketide drug with the cellular protein FKBP52 is required for acceleration of nerve cell growth.[7] A significant problem in using polyketide drugs for treatment of nerve injury is that other cellular proteins also interact with these molecules. The interaction of a polyketide with other proteins could lead to unwanted side effects. One well-characterized target for FK506 and its analogs is the protein FKBP12.[8,9] The interaction of FK506 with FKBP12, and the subsequent binding of calcineurin, leads to suppression of the immune system.[10] This is the basis for current immunosuppressive therapy using FK506 (also known as Tacrolitmus). However, long-term suppression of the immune system is undesirable while treating nerve injury.

We are interested in finding polyketide structures that show high affinity towards FKBP52 but do not interact with calcineurin. Binding studies with analogs of FK506 and available crystal structures of FKBP12 · FK506 · calcineurin complexes reveal that polyketides can be considered as built from the "binding domain" that interacts with FKBP12, the "effector domain" that interacts with calcineurin (shown boxed in Chart 1), and the cyclohexyl arm that interacts weakly with both proteins.[10,11] The structure of the binary FK506 · FKBP12 complex reveals that the pipecolinyl ester moiety and the α-ketoamide portion of the binding domain make
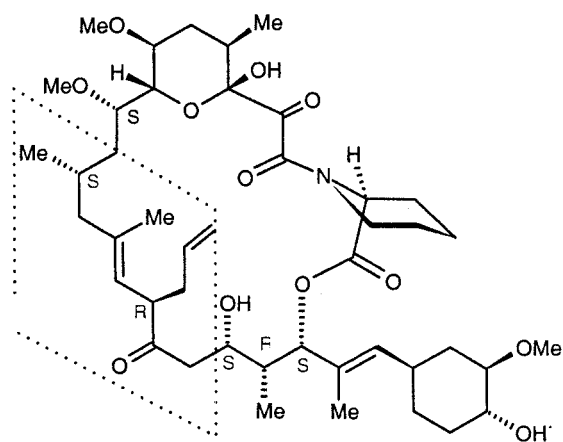

Chart 1

numerous favorable interactions with the FKBP12 protein.[11,12] The effector domain is not necessary for the polyketide to interact with FKBP52, and various compounds lacking this linker region have been suggested as possible neuroregenerative drugs.[13–15] One shortcoming of drug candidates considered so far is that they can adopt a multitude of conformations, of which many are not complementary with the binding site of FKBP52. In addition, many acyclic ligands bind to FKBP12 with a conformation that minimizes the amount of exposed hydrophobic surface area, a phenomenon called hydrophobic collapse.[11] As a result, most acyclic analogs show lower affinity towards FKBP12 than FK506 does.[11] Also, the acyclic analogs of FK506 may require complicated organic synthesis.

Studies with macrocyclic analogs of FK506 have shown that many modifications in the effector domain abolish the interaction with calcineurin while retaining a submicromolar affinity toward FKBP12. The comparison with FK506, which has a dissociation constant of 0.4 nM from FKBP12,[16] shows that further improvement of the binding affinity should be possible. The macrocyclic polyketides are especially promising candidates for neuroregenerative drugs because recent advances in identification and cloning of polyketide synthase genes make it possible to produce such polyketides via engineered biosynthesis.[3] Such an approach promises economic production of highly pure polyketides with the desired structure. In summary, the design goal for a neuroregenerative drug is a compound that shows high affinity towards FKBP52, does not interact with calcineurin, has a favorable solubility profile, and can be synthesized economically via engineered biosynthesis.

In this article we have investigated which macrocyclic polyketide structures would bind strongly to FKBP52 but not interact with calcineurin. In principle, at least two approaches are possible for designing such compounds. In the first approach, one could try to design molecules that bind strongly to FKBP52 and do not interact with FKBP12. This approach is difficult because the binding domains of FKBP12 and FKBP52 are fairly similar. FKBP52 is a 458 amino acid protein containing an N-terminal domain that shares 49% amino acid sequence homology with FKBP12.[17] Also, the three-dimensional folds of the two proteins

are similar and residues forming the binding pocket are highly conserved.[18] The second approach consists of a design of molecules that would bind both FKBP52 and FKBP12 but have a modified effector domain rendering them unable to bind calcineurin. We assume, in the framework of this approach, that the binding modes of FK506 to the proteins FKBP12 and FKBP52 are similar. In this case, the problem reduces to finding polyketide structures that have low energy conformations with the binding domain maximally similar to the binding domain of the bound FK506. The viability of this approach has been demonstrated by evaluating the conformational energies of rapamycin analogs using the MM3 force field.[19] In their work, Adalsteinsson and Bruice[19] first performed a conformational search of three molecules (templates) corresponding to the unsubstituted triketide, tetraketide, and pentaketide, respectively. Next, they calculated single point potential energies for a large number of substituted templates and identified structures that have low energy conformers similar to the conformation of the bound FK506. We now report an extension of this approach that allows a rapid conformational search with complete minimization of realistic polyketides as opposed to idealized templates.

Computer modeling of biomolecular systems and large organic molecules is currently dominated by molecular mechanics calculations due to the advantage in speed. Several high quality force fields, such as AMBER,[20,21] CFF,[22,23] CHARMM,[24,25] COMPASS,[26] GROMOS,[27] SPASIBA,[28] MM3,[29] MM4,[30] OPLS–AA,[31] and MMFF94[32,33] have been developed and are commonly used for elucidating structures and properties of molecules in gas, liquid, and crystal phases. Currently, each force field has significant strength in the area where it was specifically parameterized, that is, MMFF94 performs well for predicting the structures and relative conformational energies of a wide range of organic molecules while the OPLS–AA potential is well suited for describing intermolecular interactions.[32,34] Because we are also interested in accurately predicting relative binding free energies of polyketides to target proteins via simulation methods, we chose the OPLS–AA force field for the conformational analysis. This force field has been developed in the laboratory of William L. Jorgensen over the course of several years and has been described in detail.[31] In short, the energy of a molecular system is derived as the sum of bond stretching, bond bending, torsional, and nonbonded terms. The bond stretching and bending parameters come mostly from Weiner's 1986 AMBER force field,[20] with the exception of alkane parameters that have been adopted from CHARMM. The atomic charges and Lennard–Jones parameters have been fitted to reproduce the densities, heats of vaporization, and free energies of hydration of a wide range of organic compounds.[31,35–37] In some instances, fitting to electrostatic potential has been used to assign atomic charges.[38] Also, *ab initio* calculations of intermolecular energies of dimers or molecular hydrates in the gas phase have been used for determination of nonbonded parameters.[35,38] Most torsional parameters in the OPLS–AA force field were derived based on HF/6-31G* calculations on model compounds.[37,38] More recently, calculations at DFT or MP2 level of theory have been employed to parameterize carbohydrates,[39] perfluoroalkanes,[40] and peptides.[41]

In the course of calculating the conformations of polyketides, it became clear that in several cases the torsional parameters were
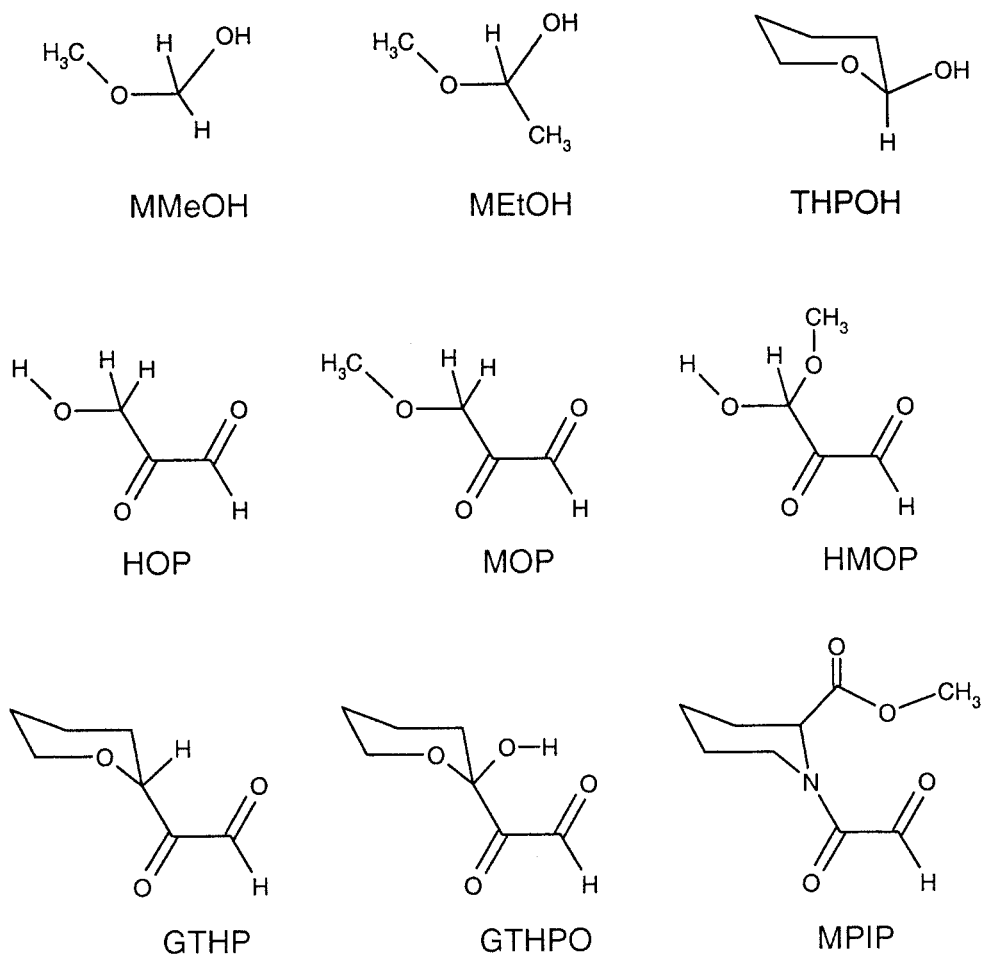
Chart 2

lacking or were not sufficiently accurate in order to predict the correct order of conformer stabilities or the magnitude of torsional barriers. We believe that the HF/6-31G* model, which was used for deriving torsional parameters in OPLS–AA, may not be adequate for describing torsional profiles of larger flexible molecules where dispersion interactions become important. Electron correlation effects tend to stabilize folded conformers over extended forms; for example, the *trans-gauche* energy difference in butane is predicted to be 1.01 kcal/mol from the HF/6-31G* calculations while the recently determined Born-Oppenheimer limit is 0.62 kcal/mol.[42] The weak performance of HF/6-31G* and also MP2/6-31G* methods for conformational energies has been noted previously. For example, Halgren has reported that HF/6-31G* calculations deviate, on average, 0.72 kcal/mol from the experimental values when conformer energies for a wide range of organic compounds are compared.[32] On the other hand, MP2 calculations with the cc-pVTZ(-f) basis set were shown to yield conformational energy differences with RMSD versus experiment of 0.35 kcal/mol.[32] To remedy this weakness of the OPLS–AA force field, we have carried out high-level *ab initio* conformational analysis of several alkanes, alcohols, ethers, hemiacetals, esters, and dicarbonyl compounds. We chose to use the augmented cc-pVTZ basis set for conformational analysis because the diffuse functions may be important for conformational energies in molecules with lone electron pairs.[43] It was subsequently found that parameterization of the intramolecular portion of the force field alone was not sufficient, and thus we modified some nonbonded parameters as well. The new nonbonded parameters were tested and refined by performing Monte Carlo simulations of bulk organic compounds. We observed an overall improvement in predicting both the bulk properties and conformational energies. With the current parameterization, the OPLS–AA force field can be successfully used for conformational analysis of complex organic molecules containing the hydroxy-, alkoxy-, ester-, and dicarbonyl substituents in saturated aliphatic chains or rings.

Methods

Ab Initio Calculations

Ab initio calculations using the program Gaussian98[44] were performed to locate minima and saddle points in the conformational energy surface of ethane, propane, isobutane, pentane, isopentane,

Table 1. Comparison of *Ab Initio* (MP2/aug-cc-pVDZ and MP2/TZ//DZ) and OPLS-AA Conformational Energies and Rotational Barriers.

Compound (Conf.)[a]	DZ	TZ//DZ	Other Data	OPLS-AA
Alkanes				
Ethane (s_{TS}-a)	3.02	2.90	2.89[TZ]; 2.88–2.90[exp50]; 2.79[ai51]	2.84
Propane (S_{TS}-a)	3.23	3.20	3.19[TZ]; 3.01[TZ+ZPVE]; 3.26[exp64]	3.08
Butane (g-a)	N/A	N/A	0.62[ai42]; 0.67 ± 0.10[exp65]	0.71
Butane (e_{TS}-a)	N/A	N/A	3.31[ai42]; 3.62 ± 0.06[exp65]	3.30
Butane (s_{TS}-a)	N/A	N/A	5.50[ai42]	5.13
Isobutane (s_{TS}-a)	3.62	3.53	3.52[TZ]; 3.90[exp66]	3.39
Pentane (ag-aa)	0.49	0.52	0.46[exp67]; 0.76[ai68]	0.81
Pentane (gg-aa)	0.67	0.69	1.36[ai68]	1.48
Isopentane (g-t)	0.83	0.75	0.81[exp69]	0.54
Isopentane (e_{TS}-t)	3.01	3.07	NA	2.74
Isopentane (s_{TS}-t)	5.39	5.31	NA	4.68
Neopentane (s_{TS}-a)	4.12	3.90	4.29[exp70]	3.88
2,2-Dimethylbutane (s_{TS}-a)	5.12	5.02	4.50[exp71]; 5.20 ± 0.20[exp72]	4.63
Cyclohexane (ch-tw.bt)	N/A	N/A	6.90[ai52]	7.01
Cyclooctane (crown-bt.ch)	N/A	N/A	1.72[ai53]	0.79
Cyclooctane (tw.bt.ch-bt.ch)	N/A	N/A	1.73[ai53]	1.76
Methylcyclohexane (ax-eq)	N/A	N/A	1.76[exp54]	1.64
Methylcyclohexane (CH_3:eq)	N/A	N/A	3.01[ai54]	3.40
Methylcyclohexane (CH_3:ax)	N/A	N/A	2.42[ai54]	3.30
Alcohols				
Methanol (s_{TS}-a)	1.15	1.00	1.065[exp73,74]	1.03
Ethanol (g-a)	0.26	0.22	0.13[exp75]; 0.05[ai76]	0.29
Ethanol (s_{TS}-a)	1.53	1.32	1.27[exp75]; 1.26[ai76]	1.48
Ethanol (e_{TS}-a)	1.30	1.15	1.15[exp75]; 1.15[ai76]	1.07
Ethanol (CH_3:a)	3.39	3.30	3.39[exp75]; 3.31[ai76]	3.20
1-Propanol. GM is g⁻a with CC—CO −62.6° and CC—OH 179.5. Figure 1.				
1-PrOH (aa-g⁻a)	0.23	0.17	0.16[TZ]	−0.34
1-PrOH (g⁻g⁻-g⁻a)	0.26	0.20	0.19[TZ]	−0.30
1-PrOH (ag-g⁻a)	0.35	0.22	0.21[TZ]	−0.13
1-PrOH (g⁻g⁺-g⁻a)	0.34	0.23	0.22[TZ]	0.03
1-PrOH (sa_{TS}-g⁻a)	5.31	5.11		4.85
1-PrOH (ea_{TS}-g⁻a)	3.61	3.35		3.40
1-PrOH (g⁻e⁺$_{TS}$-g⁻a)	1.08	0.82		0.86
1-PrOH (g⁻e⁻$_{TS}$-g⁻a)	1.16	0.96		1.05
1-PrOH (sg⁻$_{TS}$-g⁻g⁻)	5.18	4.98		4.45
1-PrOH (e⁺g⁻$_{TS}$-g⁻g⁻)	3.94	3.72		3.33
1-PrOH (e⁻g⁻$_{TS}$-g⁻g⁻)	3.75	3.52		3.60
1-PrOH (as_{TS}-aa)	1.37	1.08		1.40
1-PrOH (ae_{TS}-aa)	1.20	0.95		1.03
1-PrOH (CH_3:aa)	2.70	2.64	2.73 ± 0.06[exp77]	2.45
2-Propanol. GM is *gauche* (g) with HC-OH dihedral of ±62.6°				
2-PrOH (a-g)	0.36	0.35	0.28[exp32]; 0.45 ± 0.22[exp78]	0.28
2-PrOH (s_{TS}-g)	1.39	1.33		0.80
2-PrOH (e_{TS}-g)	1.36	1.18		1.21
2-PrOH (CH_3:g)	3.09	3.30		3.44
tert-Butanol (s_{TS}-a)	1.34	1.21	1.27[exp79]	0.96
tert-Butanol (CH_3:a)	3.55	3.46		3.77
(S)-2-Butanol. GM is *anti-anti* (aa) with CC-CC 180.0 and C_{CH2}C—OH 180.0. Figure 2.				
2-ButOH (ag⁻-aa)	0.12	0.06	−0.14[ai80,81]	−0.60
2-ButOH (ag⁺-aa)	0.36	0.28	−0.18[ai80,81]	0.03
2-ButOH (g⁻g⁻-aa)	0.40	0.32	0.65[ai80,81]	0.28
2-ButOH (g⁻a-aa)	0.50	0.44	0.73[ai80,81]	0.36
2-ButOH (g⁺g⁻-aa)	0.71	0.60	0.97[ai80,81]	0.52
2-ButOH (g⁻g⁺-aa)	0.79	0.64	0.61[ai80,81]	0.55
2-ButOH (g⁺a-aa)	0.77	0.70	1.13[ai80,81]	0.80
2-ButOH (g⁺g⁺-aa)	1.27	1.05	1.24[ai80,81]	0.48

Table 1. (continued)

Compound (Conf.)[a]	DZ	TZ//DZ	Other Data	OPLS-AA
2-ButOH (g$^+$g$^+$-aa)	1.27	1.05	1.24[ai80,81]	0.48
Cyclohexanol (eq/CS-eq/C1)	0.21	0.26	0.18[ai32]	0.14
Cyclohexanol (ax/C1-eq/C1)	0.36	0.45	0.33[ai32]; 0.58[exp32]	1.07
Cyclohexanol (ax/CS-eq/gC1)	1.20	1.20	1.14[ai32]	0.21
Ethers				
Dimethyl ether (s$_{TS}$-a)	2.60	2.62	2.69[exp82]; 2.60[exp83]	2.52
Ethyl methyl ether. GM is *anti* with CC-OC 180.0°.				
EME (g-a)	1.29	1.37	1.23[exp84]; 1.35[ai56]	1.26
EME (s$_{TS}$-a)	6.25	6.39	7.05[ai56]	6.69
EME (e$_{TS}$-a)	N/A	N/A	2.58[ai56]	2.42
EME (C-CH$_3$:a)	3.16	3.08	3.08[exp85]; 3.14[exp86]	3.04
EME (O-CH$_3$:a)	2.51	2.44	2.61[exp85]; 2.46[exp86]	2.52
Methyl propyl ether. GM is ga with CC-CO at 62.4° and CC-OC −179.1°. Figure S2.				
MPE (aa-ga)	0.32	0.26		0.02
MPE (gg-ga)	1.00	1.13		1.13
MPE (ag-ga)	1.45	1.53		1.31
MPE (sa$_{TS}$-ga)	5.01	5.04		4.37
MPE (ea$_{TS}$-ga)	3.44	3.41		3.05
MPE (as$_{TS}$-ga)	6.37	6.52		6.86
DEE (ag-aa)	1.22	1.36	1.15[exp67]	1.31
DEE (gg-aa)	2.49	2.78		2.60
Isopropyl methyl ether. GM has C1 symmetry with CC-OC 68.4° and −169.4°.				
IME (g-a)	1.92	2.54		1.81
IME (O-CH$_3$:a)	1.80	N/A	1.73[exp87]	2.11
Oxane (tw.bt-chair)	5.57	5.65	5.64[ai58]	7.07
Dimethoxyethane (asa$_{TS}$-aaa)	N/A	N/A	9.51, 8.90[ai59]	9.11
Dimethoxyethane (aga-aaa)	N/A	N/A	0.51, 0.15[ai59]	0.38
Hemiacetals				
Methoxymethanol. GM is g$^+$g$^+$ with CO-CO at 67.5° and OC-OH at 64.7. Figure S3.				
MMeOH (g$^-$g$^+$-g$^+$g$^+$)	2.09	2.09	2.05[TZ], 2.8[ai88]	2.15
MMeOH (ag$^+$-g$^+$g$^+$)	2.73	2.62	2.64[TZ], 3.3[ai88]	2.58
MMeOH (sg$^+$$_{TS}$-g$^+g^+$)	7.14	7.09		7.24
MMeOH (aa$_{TS}$-g$^+$g$^+$)	6.54	6.43	6.42[TZ], 8.2[ai88]	6.52
MMeOH (O-CH$_3$:g$^+$g$^+$)	1.65	1.51		1.88
MMeOH (O-CH$_3$:aa)	2.31	2.30		1.97
(*R*)-1-Methoxyethanol. GM is g$^-$t with CCOH −55°, and CC-OC −171°. Figure 4.				
MEtOH (tg$^+$-g$^-$t)	1.27	1.45		1.48
MEtOH (tt-g$^-$t)	1.79	1.77		1.85
MEtOH (tg$^-$-g$^-$t)	2.62	2.59		3.59
MEtOH (gg$^-$-g$^-$t)	3.80	3.70		3.50
MEtOH (gg$^+$-g$^-$t)	4.21	4.24		3.79
MEtOH (C-CH$_3$:g$^-$t)	3.22	3.22		3.11
MEtOH (C-CH$_3$:tt)	2.80	2.80		3.12
(*S*)-Tetrahydropyran-2-ol. GM is axial *gauche* (ax/g$^+$) with CO-CO 64.4° and OC-OH 56.7°. Figure 5.				
THPOH (eq/g$^+$-ax/g$^+$)	1.15	N/A	1.3[ai88]	1.43
THPOH (eq/g$^-$-ax/g$^+$)	1.89	N/A	2.2[ai88]	1.55
THPOH (ax/g$^-$-ax/g$^+$)	3.01	N/A	4.0[ai88]	1.62
THPOH (ax/a-ax/g$^+$)	3.65	N/A	4.4[ai88]	3.55[TS]
THPOH (eq/a$_{TS}$-ax/g$^+$)	5.28	N/A		5.57[TS]
Esters				
Methyl formate (E-Z)	5.48	5.45	5.45[TZ]; 4.75 ± 0.19[exp89]; 5.65[ai32]	4.50
Methyl formate (O-CH$_3$:Z)	1.25	1.12	1.11[TZ]; 1.21[exp] 1.19[exp60]	1.21
Methyl acetate (E-Z)	7.33	7.47	8.5 ± 1.0[exp89]	8.11
Methyl acetate (C-CH$_3$:Z)	0.20	0.19	0.29[exp61]	0.27
Methyl acetate (O-CH$_3$:Z)	1.37	1.17	1.22[exp61]	1.24
Methyl propionate (E-Z)	N/A	N/A	8.75[ai90]	8.33
Methyl propionate (O-CH$_3$:Z)	1.36	1.17		1.26

Table 1. (continued)

Compound (Conf.)[a]	DZ	TZ//DZ	Other Data	OPLS-AA
Methyl propionate (C-CH$_3$:Z)	2.51	2.47		2.33
Ethyl formate (Ea-Za)	5.10	5.06	3.2[exp91]	4.00
Ethyl formate (Zg-Za)	N/A	N/A	0.19 ± 0.6[exp92]; 0.34[ai32]	0.24
Ethyl acetate (Zg-Za)	N/A	N/A	0.32[exp93]	0.25
Isopropyl formate (Zg-Za)	2.35	2.42	2.43[ai94]	2.96
Isopropyl formate (Ea-Za)	4.71	4.61		3.64
Isopropyl formate (Eg-Za)	6.99	7.00		5.83
Propyl formate (Zga-Zag)	0.03	0.09		0.23
Propyl formate (Zg$^+$g$^+$-Zag)	−0.01	0.14		0.05
Propyl formate (Zaa-Zag)	0.25	0.22		0.08
Glyoxal derivatives				
3-Hydroxy-2-oxopropanal. Figure 8.				
HOP (tgg-tee)	1.97	2.36		2.52
HOP (tea-tee)	3.83	4.17		4.14
HOP (tg$^+$g$^-$-tee)	4.24	4.79		4.31
HOP (cee-tee)	4.52	4.31		5.12
HOP (cta-tee)	7.42	7.79		6.54
HOP (cea-tee)	9.30	9.45		9.86
3-Methoxy-2-oxopropanal. Figure 9.				
MOP (tea-teg)	0.92	0.72		0.72
MOP (tg$^-$g$^+$-teg)	1.18	1.51		1.11
MOP (tg$^+$a-teg)	1.33	1.39		1.18
MOP (cg$^-$g$^+$-teg)	3.28	3.25		1.38
MOP (caa-teg)	4.18	4.03		3.40
MOP (ceg-teg)	5.17	5.01		4.96
MOP (cea-teg)	6.29	5.89		6.19
3-Hydroxy-3-methoxy-2-oxopropanal. Figure S4.				
HMOP (Conf2-Conf1)	0.47	0.55		1.76
HMOP (Conf3-Conf1)	1.98	2.23		2.33
HMOP (Conf4-Conf1)	3.56	3.43		2.32
HMOP (O-CH$_3$:Conf1)	1.82	1.75		1.83
2-Glyoxoyl-tetrahydropyran. Figure S5.				
GTHP (Conf2-Conf1)	0.03[G]	N/A		−0.23
GTHP (Conf3-Conf1)	0.57[G]	N/A		1.10
GTHP (Conf4-Conf1)	2.68[G]	N/A		2.31
2-Glyoxoyl-tetrahydropyran-2-ol. Figure S6.				
GTHPO (Conf2-Conf1)	1.38[G]	N/A		0.78
GTHPO (Conf3-Conf1)	3.46[G]	N/A		−0.12
GTHPO (Conf4-Conf1)	4.63[G]	N/A		3.20
GTHPO (Conf5-Conf1)	5.22[G]	N/A		3.38
GTHPO (Conf6-Conf1)	7.40[G]	N/A		3.78

Energies (in kcal/mol) are given relative to the global minimum (GM).

[a]The following symbols, based on a recent recommendation,[95] are used to define the conformers and torsional barriers: a—anti ($\theta = 180°$); e—eclipsing ($\theta \approx \pm120°$); g—gauche ($\theta \approx \pm60°$); s—*syn* ($\theta = 0°$); t—transoid ($\theta \approx \pm165°$); CH$_3$:a—barrier for the rotation of a terminal methyl group in the anti conformer. Conformations of cyclic structures are designated as: ch—chair; tw—twist; bt—boat; eq—substituent occupies an equatorial position; ax—substituent occupies an axial position. The symbols C1 and CS indicate molecular symmetry. The rotation around the O=C(sp^2)—O(sp^3)—C(sp^3) dihedral in esters is described using symbols Z (cis, 0°) and E (trans, 180°). The bond involved in the methyl group rotation in esters is explicitly shown, that is, O—CH$_3$:Z designates a rotation of the methoxy group in the Z conformer. A subscript TS in the first column indicates that the structure corresponds to the top of the rotational barrier, the superscript TZ indicates that both energy evaluation and optimization were performed at the MP2/aug-cc-pVTZ level, and superscript G designates optimization with the 6-31+G(d,p) basis.

neopentane, 2,2-dimethylbutane, methanol, ethanol, 1-propanol, 2-propanol, *sec*-butanol, *tert*-butanol, cyclohexanol, ethyl methyl ether (EME), diethyl ether (DEE), methyl propyl ether (MPE), isopropyl methyl ether (IME), oxane, methoxymethanol (MMeOH), methoxyethanol (MEtOH), tetrahydropyran-2-ol (THPOH), 3-hydroxy-2-oxopropanal (HOP), 3-methoxy-2-

Table 2. Suggested Nonbonded Parameters for the OPLS-AA Force Field for the Description of Alkanes, Alcohols, Ethers, Hemiacetals, and Esters.

Type	Atom	Q	σ	ϵ
Alkanes				
CT	CH_3 in alkanes	−0.135	3.52	0.067
CT	CH_2 in alkanes	−0.090	3.52	0.067
CT	CH in alkanes	−0.045	3.38	0.059
CT	C in alkanes	0.000[a]	3.20	0.051
HC	H in alkanes	0.045	2.50[a]	0.030[a]
Alcohols				
CT	CH_3 next to OH in methanol	0.170	3.52	0.067
CT	CH_2 next to OH in primary alcohols	0.200	3.52	0.067
CT	CH next to OH in secondary alcohols	0.230	3.38	0.059
CT	C next to OH in tertiary alcohols	0.260	3.20	0.051
OH	O hydroxyl in mono alcohols	−0.660	3.08	0.170[a]
HO	H hydroxyl in mono alcohols	0.400	0.00[a]	0.000[a]
HC	H alpha to hydroxyl group	0.030	2.50[a]	0.030[a]
Ethers				
CT	CH_3 next to OS in ethers	0.110[a]	3.52	0.067
CT	CH_2 next to OS in ethers	0.140[a]	3.52	0.067
CT	CH next to OS in secondary ethers	0.170[a]	3.38	0.062
CT	C next to OS in tertiary ethers	0.200[a]	3.20	0.051
OS	Ether oxygen	−0.400[a]	2.90[a]	0.140[a]
HC	H alpha to ether oxygen	0.030[a]	2.50[a]	0.030[a]
Hemiacetals				
CT	CH_2O_2 in hemiacetal	0.400	3.52	0.067
CT	$CHRO_2$ in hemiacetal	0.430	3.38	0.059
CT	CR_2O_2 in hemiacetal	0.460	3.20	0.051
OH	O hydroxyl in hemiacetals	−0.660	3.08	0.170[a]
HO	H hydroxyl in hemiacetals	0.400	0.00[a]	0.000[a]
OS	Ether oxygen in hemiacetals	−0.400[a]	2.90[a]	0.140[a]
HC	H alpha to oxygens	0.030	2.50[a]	0.030[a]
Esters (for the alkoxy moiety)				
CT	CH_3 in methyl esters	0.160	3.52	0.067
CT	CH_2 in ethyl esters	0.190	3.52	0.067
CT	CH in isopropyl esters	0.220	3.38	0.059
CT	C in *tert*-butyl esters	0.250	3.20	0.051
OE	Alkoxy oxygen in esters	−0.330[a]	3.00[a]	0.170[a]
HC	H alpha to oxygen	0.030[a]	2.42[a]	0.015[a]
Glyoxal derivatives				
CG	Carbonyl C adjacent to CT/CO	0.360[b]	3.75[a]	0.105[a]
CG	Carbonyl C adjacent to HC	0.430[b]	3.75[a]	0.105[a]
OG	Carbonyl O adjacent to CT/CO	−0.360[b]	2.96[a]	0.210[a]
OG	Carbonyl O adjacent to HC	−0.430[b]	2.96[a]	0.210[a]
HC	Hydrogen connected to GG	0.000	2.42[a]	0.015[a]

[a]Value is unchanged from the standard OPLS-AA force field value.
[b]Values are changed from our previously recommended value ± 0.40[63] based on RESP calculations and preliminary liquid simulations of glyoxal and dimethylglyoxal.

oxopropanal (MOP), 3-hydroxy-3-methoxy-2-oxopropanal (HMOP), 2-glyoxoyl-tetrahydropyran (GTHP), 2-glyoxoyl-tetrahydropyran-2-ol (GTHPO), methyl formate, methyl acetate, methyl propionate, ethyl formate, propyl formate, isopropyl formate, and a pipecolinyl ester (MPIP). The structures and the corresponding abbreviations for some of these molecules are shown on Chart 2. For molecules with complex potential energy surfaces, torsional profiles were generated by varying the torsional angle of interest in 20–40° increments and minimizing all other

degrees of freedom. All molecules were initially optimized at the MP2/aug-cc-pVDZ level and single point energies were evaluated at the MP2/aug-cc-pVTZ level (hereafter abbreviated as MP2/TZ//DZ) except THPOH, for which only MP2/aug-cc-pVDZ energies were determined. Two larger molecules, GTHP and GTHPO, were studied at the MP2/aug-cc-pVDZ//MP2/6-31+G(d,p) level. The torsional profile for the pipecolinyl ester was determined at the MP2/6-31+G(d,p) level. A comparison with available experimental data suggested that the MP2/TZ//DZ approach yields an accu-

rate description of the conformational energy surface but bond lengths are systematically overestimated. To test if this overestimation leads to errors in conformational energies, low energy conformers of ethane, propane, isobutane, methanol, ethanol, 1-propanol, 2-propanol, EME, methoxymethanol, HOP, methyl formate, methyl acetate, and ethyl formate were reoptimized at the MP2/aug-cc-pVTZ level. It has been shown previously that this level of theory predicts bond lengths with an accuracy of 0.006 Å.[45,46] The optimization with the triple-zeta basis set did not change conformational energies significantly. In some cases, the conformational energies evaluated at the MP2/aug-cc-pVDZ level were found to be significantly different compared to the MP2/TZ//DZ results (see Table 1). We also observed that the relative energies for conformers of GTHP and GTHPO showed differences up to 0.6 kcal/mol when MP2/6-31+G(d,p) optimized energies were compared to the MP2/aug-cc-pVDZ//MP2/6-31+G(d,p) results. For this reason GTHP and GTHPO data were excluded from the statistical analysis.

Force Field Parameterization

The *ab initio* data were used to reparameterize the OPLS–AA(2,2) force field to yield a better description of oxygen-containing organic compounds. The parameters were refined starting with bond stretching and bending parameters followed by optimization of nonbonded parameters and torsional force constants. All molecular mechanics calculations were performed with the program BOSS42.[47] The equilibrium bond lengths and angles were obtained by fitting the OPLS-minimized structures to MP2/aug-cc-pVTZ structures of molecules shown in Figure S1 in the Supplementary Material.

Determination of atomic charges for alcohols was based on fitting the molecular electrostatic potential to atom-centered point charges using the constraint that functional units (such as CH_3 in ethanol) carry a net zero charge. The electrostatic potential was obtained from MP2/aug-cc-pVDZ densities using the Merz-Singh-Kollman scheme with 12 layers in Gaussian98.[44,48] Potentials for several similar molecules or many conformations of one molecule were fitted simultaneously with the program RESP.[49] This method was not sufficient for unambiguous determination of charges of aliphatic hydrogens; values in the range of 0.03–0.09 gave almost similar fits. Because we found that the value of Q(H)=0.045 gives a good description of conformational energies of secondary alcohols, this value was fixed in RESP calculations during the determination of charges for the α-carbon, α-hydrogens, oxygen and hydroxyl hydrogen in alcohols.

Several van der Waals parameters for the 12–6 potential were modified based on Monte Carlo simulations of bulk liquids. Liquid simulations of cyclopentane, cyclohexane, *n*-pentane, isopentane, methanol, ethanol, 1-propanol, 2-propanol, *sec*-butanol, *tert*-butanol, oxane, isopropyl methyl ether, methyl *tert*-butyl ether, and diethyl ether were performed at room temperature in the periodic box in a manner similar to that described previously.[31] Isobutane, *n*-butane, neopentane, dimethyl ether, and ethyl methyl ether were simulated at their corresponding boiling temperatures. In our simulations, cubic boxes of at least 30 Å in length were employed that allowed use of nonbonded cutoffs of 14–15 Å. Each liquid simulation consisted of at least $4 \cdot 10^6$ configurations of equilibration and 14–$24 \cdot 10^6$ configurations of averaging. Each simulation of an isolated molecule was done by equilibrating for $2 \cdot 10^6$ conformations and averaging for at least $8 \cdot 10^6$ conformations. All molecules were fully flexible during simulations. For each molecule, 10–25 simulations were performed by varying the nonbonded parameters and the optimal parameter set was determined by fitting the calculated densities and heats of vaporization to the corresponding experimental values.

The main parameterization set for torsional force constants included MP2/TZ//DZ rotational profiles for ethane, propane, isobutane, isopentane, neopentane, 2,2-dimethylbutane, methanol, ethanol, 1-propanol, 2-propanol, tert-butanol, dimethyl ether, ethyl methyl ether, methyl propyl ether, methoxymethanol, 3-hydroxy-2-oxopropanal, 3-methoxy-2-oxopropanal, methyl formate, methyl acetate, ethyl acetate, methyl propionate, and propyl formate. Also, the relative energies of all stable conformers of pentane, *sec*-butanol, cyclohexanol, diethyl ether, isopropyl methyl ether, methoxyethanol, and isopropyl formate were included along with the data on low-energy conformers of THPOH, HMOP, GTHP, and GTHPO. This set was supplemented with reliable experimental data or recently published *ab initio* energies for ethane,[50,51] butane,[42] cyclohexane,[52] cyclooctane,[53] methylcyclohexane,[54] cyclohexanol,[32] dimethyl ether,[55] ethyl methyl ether,[56] oxane,[57,58] dimethoxyethane,[59] methyl formate,[60] methyl acetate,[61] and ethyl formate.[62] Finally, torsional profiles and conformational energies for diketones and ketoamides studied by us previously[63] were included. The OPLS–AA torsional parameters were derived by iterative fitting of OPLS–AA calculated energy profiles for rotation around single bonds to the corresponding *ab initio* energy profiles. In the later stages, conformational analysis of all molecules in the parameterization set was done, and when discrepancies occurred, refitting to torsional profiles was performed.

Conformational Analysis of Polyketides

The new parameters were used to perform conformational analysis of selected polyketides starting with a previously generated library of small rapamycin analogs.[19] We studied tri- and tetraketides corresponding to analogs of FK506 (methoxy substituent at the position 31). The stable conformers were identified using the stochastic conformational searching facility in BOSS42. For each molecule, 15,000 trial structures were generated by moving every atom with the upper bound radius of 2 Å. Three criteria were used for retaining unique conformers. To satisfy the first criterion, the energy of a given conformer had to be more than 0.01 kcal/mol different from the energy of any previous conformer. Second, the conformer had to show a RMS deviation above 0.5 Å from any previous conformer when the two structures were superimposed. Last, the sum of squared internuclear distances between all possible atom pairs in the given conformer had to be more than 4.0 $Å^2$ different from the value found in any other conformer. Structures that satisfied all three criteria and were local minima on the potential energy surface were considered to be unique conformers. The low-energy ketide structures were compared to the crystal structure of bound FK506 (PDB code 1FKF). The lowest energy conformer of the tetraketide showing the highest similarity to the drug FK506 was docked to the average solution structure of the rabbit FKBP52 (also known as FKBP59, PDB code 1ROT)[18] using the program SYBYL (Tripos, Inc.) in order to confirm its ability to fit to the binding pocket.

Table 3. Suggested Torsional Parameters for Alkanes, Alcohols, Ethers, Hemiacetals, and Esters To Be Used with New Nonbonded Parameters Based on Q(H)=0.045.

Type	V1	V2	V3	V4	Parameterization Data
Alkanes					
HC—CT—CT—HC	0.00	0.00	0.30	0.00	Ethane
HC—CT—CT—CT	0.00	0.00	0.32	0.00	Propane, isobutane, neopentane
					Butane, pentane, isopentane, cyclohexane, cyclooctane, 2,2-
CT—CT—CT—CT	0.75	0.20	0.25	−0.25	dimethylbutane
Alcohols					
HC—CT—OH—HO	0.00	0.00	0.34	0.00	MeOH, EtOH, iPrOH, cHexOH
CT—CT—OH—HO	−0.20	0.04	0.32	−0.06	EtOH, 1-PrOH, iPrOH, tBuOH, cHexOH
HC—CT—CT—OH	0.00	0.00	0.34	0.00	EtOH, iPrOH, tBuOH
CT—CT—CT—OH	1.35	−0.08	0.29	−0.04	1-PrOH, 2-BuOH, cHexOH
Ethers					
HC—CT—OS—CT	0.00	0.00	0.67	0.00	Dimethyl ether, EME, IME
CT—CT—OS—CT	−0.10	−0.10	0.70	−0.05	EME, DEE, IME, oxane
HC—CT—CT—OS	0.00	0.00	0.31	0.00	EME, DEE, MPE
CT—CT—CT—OS	0.95	−0.20	0.30	−0.25	MPE, oxane
Hemiacetals					
OS—CO—OH—HO	−0.40	−2.15	0.40	−0.35	MMeOH, MEtOH
HC—CO—OH—HO	0.00	0.00	0.34	0.00	As in alcohols, MMeOH
CT—CO—OH—HO	−0.20	0.04	0.32	−0.06	As in alcohols, MEtOH
CT—OS—CO—OH	−1.30	−1.80	1.10	0.00	MMeOH, MEtOH
HC—CT—CO—OH	0.00	0.00	0.40	0.00	MEtOH
CT—CT—CO—OH	1.35	−0.08	0.29	−0.04	As in alcohols, THPOH
HC—CT—CO—OS	0.00	0.00	0.44	0.00	MEtOH
CT—CT—CO—OS	0.95	−0.20	0.30	−0.25	As in ethers, THPOH
HC—CT—OS—CO	0.00	0.00	0.50	0.00	MMeOH
CT—CT—OS—CO	−0.10	−0.10	0.70	−0.05	As in ethers, THPOH
Esters					
HC—CT—CT—C	0.00	0.00	−0.11	0.00	Methyl propionate
CT—CT—C=O	−0.31	0.94	−0.35	0.12	Methyl propionate
CT—CT—C—OE	0.00	0.00	−0.533	0.00	Standard OPLS-AA
HC—CT—C=O	0.00	0.00	0.00	0.00	Methyl acetate
HC—CT—C—OE	0.00	0.00	0.05	0.00	Methyl acetate
CT—C—OE—CT	3.00	5.12	0.00	0.00	Methyl formate, methyl acetate, ethyl
Formate					
C—OE—CT—HC	0.00	0.00	0.08	0.00	Methyl formate, methyl acetate, methyl
Propionate					
C—OE—CT—CT	−1.60	−0.40	0.10	0.00	Ethyl formate
OE—CT—CT—HC	0.00	0.00	0.34	0.00	As in alcohols
Glyoxal analogs					
O=CG—CT/CO—OH	5.70	2.40	−1.00	0.20	HOP, HMOP, GTHPO
CG—CG—CT/CO—OH	0.00	0.00	0.00	0.00	HOP, HMOP, GTHPO
CG—CT/CO—OH—HO	−0.60	−0.50	0.70	0.00	HOP, HMOP, GTHPO, HMGP
O=CG—CT/CO—OS	0.00	0.00	0.00	0.00	MOP, HMOP, GTHP, GTHPO
CG—CG—CT/CO—OS	−3.50	2.00	0.40	0.30	MOP, HMOP, GTHP, GTHPO
CG—CT/CO—OS—CT	−2.60	−0.30	0.50	0.00	MOP, HMOP, GTHP, GTHPO
O=CG—CO—CT	0.00	0.00	0.00	0.00	GTHPO
CG—CG—CO—CT	−2.00	0.75	0.40	0.00	GTHPO

Results

Structures and Conformational Barriers in Model Compounds

The MP2/aug-cc-pVTZ optimized structures of low energy conformers for some alkanes, alcohols, ethers, hemiacetals, and esters are shown in Figure S1 (Supplementary Material). The MP2/aug-cc-pVTZ optimized geometries are in very good agreement with experimental structures in cases where a comparison is available while the MP2/aug-cc-pVDZ method systematically overestimates the length of carbon–oxygen bonds.

Table 1 lists the *ab initio* conformational energies for compounds that were used for the determination of torsional force

Table 4. Properties of Bulk Liquids.

Liquid	T, °C	NMOL	R	V_{calc}	V_{exptl}[a]	$\Delta H_{vap,calc}$	$\Delta H_{vap,expt}$[b]
n-Butane	−0.54	282	14	161.4	160.6	5.58	5.36
n-Pentane	25.00	267	14	194.3	192.7	6.53	6.32
Isobutane	−12.00	332	14	159.0	162.3	5.36	5.09
Isopentane	25.00	267	15	196.6	194.5	6.08	5.94
Neopentane	9.50	267	14	193.1	198.9	5.82	5.44
Cyclopentane	25.00	267	15	160.8	161.7	6.85	6.83
Cyclohexane	25.00	267	14	182.6	180.64	8.02	7.90
Methanol	25.00	539	14.5	68.4	67.66	8.92	8.94
Ethanol	25.00	371	15	96.5	97.43	10.15	10.13
1-Propanol	25.00	300	15	124.8	124.80	11.16	11.34
2-Propanol	25.00	333	15	126.4	127.77	10.82	10.85
sec-Butanol	25.00	267	15	153.8	153.05	11.78	11.91[c]
tert-Butanol	25.00	267	15	153.8	157.47	11.22	11.16
Dimethyl ether	−24.80	375	15	106.3	104.1	5.39	5.14
Ethyl methyl ether	7.35	293	14	140.2	138.5	6.15	5.91
Isopropyl methyl ether	25.00	267	14	175.0	173.65	6.36	6.31
Methyl *tert*-Butyl ether	25.00	267	15	201.6	199.12	7.12	7.13
Diethyl ether	25.00	267	14	173.2	173.94	6.93	6.48
Oxane	25.00	267	15	164.5	162.74	8.56	8.35

Comparison of OPLS-AA molecular volumes (Å^3 per molecule) and heats of vaporization (kcal/mol) with the experimental data.

[a]Experimental densities were taken from the following sources: alcohols—ref. 96; isobutane—extrapolated from data in ref. 97; neopentane—extrapolated from data in ref. 98; cyclohexane and oxane—ref. 99; aliphatic ethers—ref. 100, except dimethyl ether data which were taken from refs. 101 and 102.

[b]Experimental heats of vaporization were obtained from the NIST WebBook.[103]

[c]Experimental ΔH_{vap} is probably for the racemic mixture while calculations were performed with pure isomer. However, ΔH_{vap} for the pure isomer is expected to be very close to the value of the racemic mixture as the densities and boiling points of the two liquids are nearly identical.

constants. For comparison, data from previously published research and results of OPLS–AA calculations with newly optimized parameters are also given. When comparing the experimental and calculated data one should remember that *ab initio* torsional barriers correspond to the energy difference between the saddle point and the bottom of the potential well while the experimental data usually contain the contribution of zero point energy (ZPVE).

Force Field Parameters

Minimization of molecules shown in Figure S1 (Supplementary Material) using standard OPLS–AA parameters revealed that the bond stretching parameters can be improved by introducing individual bond length parameters for the carbon–oxygen single bond in alcohols, ethers, and esters. The standard parameter set assigned
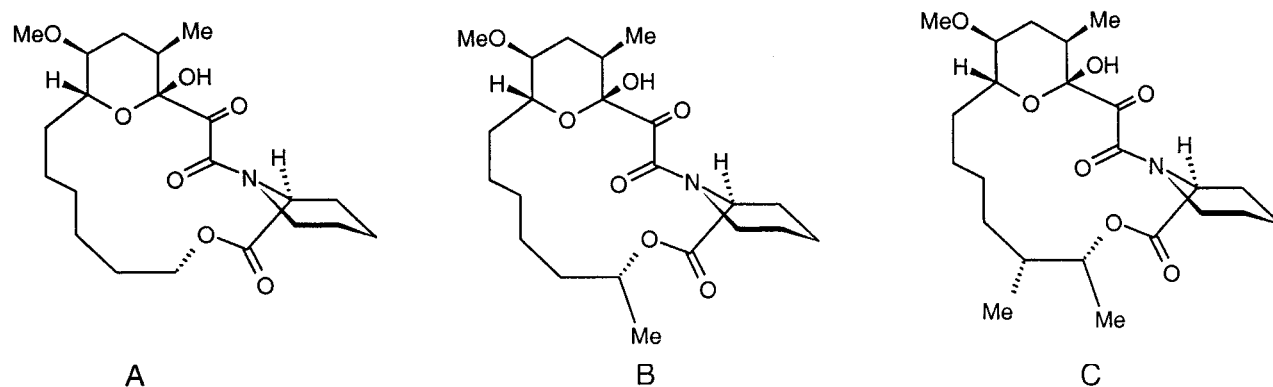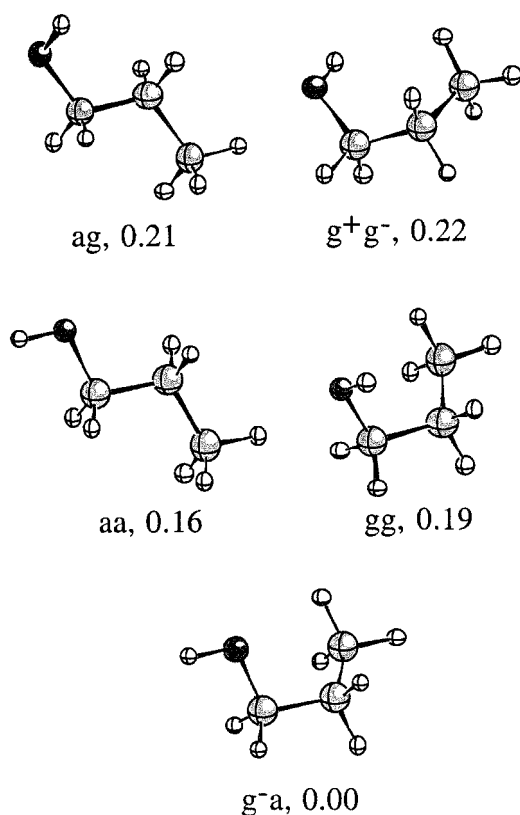

Chart 3

Figure 1. Conformers and their relative energies (in kcal/mol) of 1-propanol at the MP2/aug-cc-pVTZ//MP2/aug-cc-pVTZ level.

a common distance, 1.41 Å, to all such bonds; this is too short for alcohols and esters. Optimal C—O distances were 1.423 Å for alcohols, 1.409 Å for ethers, and 1.437 Å for esters. The optimal lengths for the CT—OH and CT—OS bonds in hemiacetals were 1.404 Å, and 1.390 Å, respectively. Standard bond bending parameters were found to be appropriate in most cases, and only some small adjustments of equilibrium angles were made. The CT-OH-HO angle was reduced from 108.5 to 108.2°, and the CT-CT-OH angle was changed from 109.5 to 108.5° in order to improve agreement for alcohols. In addition, the CT-OS-CT angle in ethers was reduced from 109.5 to 108.6°. Values of 106.2 and 109.5° were assigned for CG-CT-OS and CG-CT-OH angles, respectively, to describe glyoxal derivatives.

Reproduction of *ab initio* conformational energies of some cyclic molecules, such as cyclooctane, cyclohexanol, tetrahydropyran-2-ol, 2-glyoxoyl-tetrahydropyran, and 2-glyoxyl-tetrahydropyran-2-ol, was not successful with the standard OPLS–AA parameters. For cyclohexanol, standard OPLS–AA predicts the axial conformer with C_s symmetry to be the most stable, but *ab initio* calculations show that this conformer has the highest energy. The discrepancy in relative energies of the axial C_s and equatorial C_1 conformers was 2.03 kcal/mol. Cyclohexanol is a challenging molecule for force fields that use appreciable positive charges on aliphatic hydrogens.[32] After adjustments of torsional force constants failed to improve the agreement we investigated if the

reduction of Q(H) from its standard value of 0.06 or changing the scaling factor for 1-4 electrostatic interactions would improve the calculated conformational energies. It was found that the reduction of the hydrogen charge to 0.045 improved the agreement between OPLS–AA and *ab initio* results for secondary alcohols as well as for cyclic alkanes. Change of the charge of the aliphatic hydrogen, which is one of the basic parameters of the OPLS–AA force field, necessitated extensive redetermination of other force field parameters. Based on RESP calculations we adjusted charges of the hydroxyl oxygen and the hydroxyl hydrogen to −0.66 and +0.40, respectively. In addition, the charge on hydrogens adjacent to an sp^3 oxygen was decreased further to 0.03. In the standard OPLS–AA force field such hydrogens had either charge of 0.10 (hemiacetals), 0.06 (most alcohols), 0.04 (methanol), or 0.03 (ethers, esters).[31,37] Bulk liquid simulations of primary alcohols, ethers, unbranched alkanes, and cycloalkanes indicated that only minor adjustments of σ_C and ε_C values were necessary. Excellent fit to experimental bulk liquid data was obtained after increasing σ_C from 3.50 to 3.52 and raising ε_C from 0.066 to 0.067. However, agreement for branched molecules was still not satisfactory. After noting that larger errors for branched molecules occurred with the original OPLS–AA force field as well,[31] we decided to introduce unique nonbonded parameters for secondary and tertiary sp^3 carbons. Concurrent optimization of nonbonded parameters and torsional force constants yielded final values shown in Tables 2 and 3. The predicted relative conformational energies are listed in the last column of Table 1 and bulk liquid densities and heats of vaporization are given in Table 4.

Conformation of Polyketides

The conformational search was performed for three tetraketides (Chart 3) as well as for a triketide with unsubstituted linker region. In the current article we follow the previously used terminology where the prefix "tetra" refers to the number of ketide units in the linker region. For comparison, the linker in FK506 is built from seven ketide units.[104] It should be noted that the biosynthesis of tetraketides B and C is in principle possible using acetate as a starter unit while the enzymatic synthesis of tetraketide A is not feasible. The conformational search of a three tetraketide yielded several hundred conformers for each structure spanning nearly 20 kcal/mol. Despite this structural diversity, the low energy conformers for these molecules were remarkably similar. All of the low energy conformations were characterized by a planar amide group in the trans conformation and by a nearly orthogonal dicarbonyl moiety. The two carbonyl groups were significantly more orthogonal in tetraketides (110° vs. 142°) than in similar acyclic models,[63] suggesting that a requirement to maintain the covalent ring structure puts a significant torsional stress to the dicarbonyl moiety. The pipecolinyl and pyranosyl rings adopt chair conformations with 11-methyl and 13-methoxy groups in equatorial positions. More importantly, the low energy conformers of these tetraketides were very close to the bound conformation of FK506, suggesting that tetraketides where the linker domain is replaced by a simple aliphatic chain would exhibit significant affinity toward proteins FKBP12 or FKBP52. Docking of the lowest energy conformer of tetraketide **C** to the binding pocket of the rabbit FKBP52 was achieved using the crystal structure of FKBP12–FK506 as a guide.
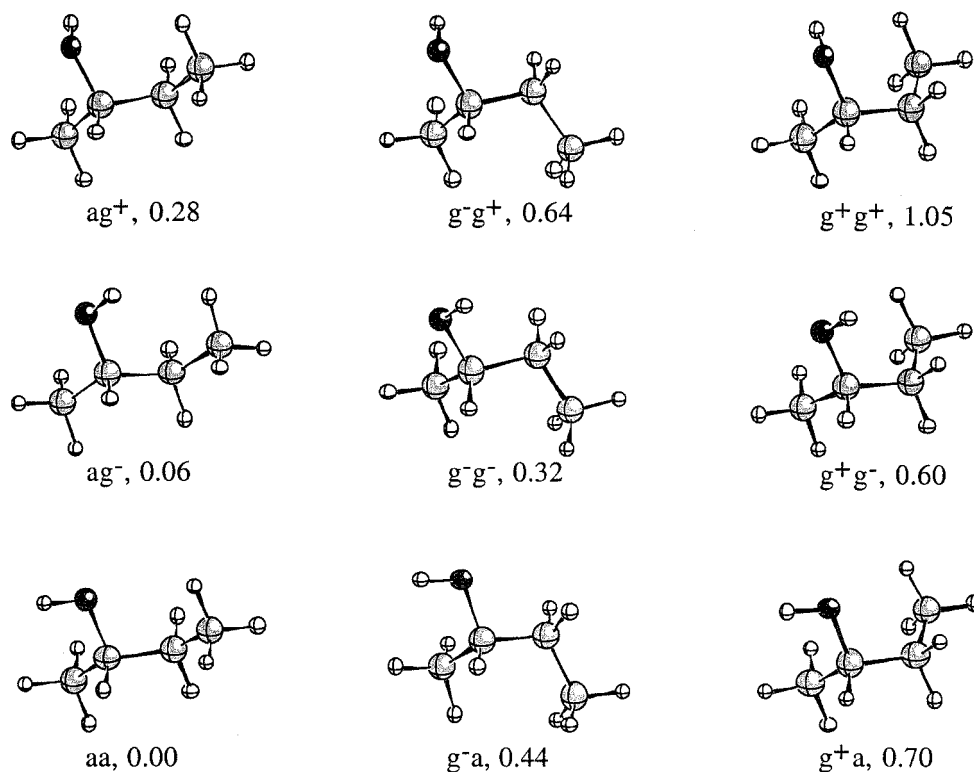
Figure 2. Conformers and their relative energies (in kcal/mol) of 2-butanol at the MP2/TZ//DZ level.

Discussion

Structural Trends from MP2 Calculations

The MP2 calculations suggest that the length of the carbon–oxygen single bond in R_1—O—R_2 depends in a systematic way on the nature of substituents R_1 and R_2. For a constant R_2, the length increases in the series methyl < ethyl < isopropyl < *tert*-butyl. This trend is consistent with the experimental results for alcohols, ethers, and esters,[79,106,107] and can be rationalized as a sum of steric and inductive effects. For a constant R_1 the bond length increases in the series hemiacetal < ether < alcohol < ester. It was also found that the carbon–carbon bond adjacent to an sp^3 oxygen is

considerably shorter than similar bonds in hydrocarbons. For example, the C—C distance in ethanol was calculated at 1.504 Å (experimental distance of 1.512 Å has been reported)[108] while this distance in propane was calculated at 1.524 Å (expt. r_s 1.526 Å).[109] Similar shortening of the carbon–carbon bond was also observed for hemiacetals ($r_{C—C}$ is 1.509 Å in 1-methoxyethanol), ethers ($r_{C—C}$ is 1.512 Å in ethyl methyl ether), and esters ($r_{C—C}$ is 1.501 Å in ethyl formate). The implication of these results is that force fields that do not allow shrinkage of the C—C bond upon substitution with the electronegative element overestimate this bond length.

Conformational and Structural Data for Individual Molecules

Many molecules from this study have been investigated in detail previously so we will give here only a brief summary of the most interesting results.

Alcohols

Our results for methanol and ethanol are in good agreement with previous experimental and high-level computational results.[74–76,108,110–112] *n*-Propanol has five distinct conformers which have been studied previously at the MP2/6-31+G(d) and MP4SDQ/TZP levels.[88,94] Current MP2/aug-cc-pVTZ optimization predicts, in agreement with previously published results, that the lowest energy conformer is gauche-anti (Fig. 1). However, the four remaining conformers are very close in energy and present

results do not allow definite ordering of *n*-propanol conformers. Because the highest energy conformer lays only 0.23 kcal/mol above the global minimum, it is likely that all conformers are present in significant amounts at room temperature. Isopropanol has two stable conformations, designated here as gauche (a.k.a. synclinal, where HC—OH is ±63.6°) and anti (a.k.a. antiperiplanar, with HC—OH = 180°). The gauche conformer is more stable than the anti form but the relative energy of conformers is not precisely known.[113] The MP2/aug-cc-pVTZ optimization predicts that the anti conformer lays 0.27 kcal/mol above the gauche form, in agreement with previously reported theoretical values.[94] 2-Butanol (Fig. 2) exists in nine conformers, which have been recently studied at the B3LYP/6-31G(d) level.[80,81] Our results confirm that all nine conformers are present in significant amounts at room temperature, but the identity of the global minimum remains elusive. The MP2/TZ//DZ calculations predict that the *aa* conformer is the most stable, followed closely by the *ag⁻* conformer, while DFT calculations predict that the *ag⁺* form is the global minimum. This molecule is an important model for the C—C—C—O moiety in C-glycosides and further studies of its conformational properties may be necessary.

Ethers

Ethyl methyl ether has two stable conformers and experimental estimates for the anti-gauche energy difference range from 1.11 to 1.5 kcal/mol.[56,85] This molecule has been well studied by *ab initio* calculations,[56,94] and our MP2/TZ//DZ value, 1.37 kcal/mol, is very close to the best available estimate, 1.36 kcal/mol at the CCSDT/6-311G(d) level.[56] The calculated barrier for the C—CH₃ rotation, 3.08 kcal/mol, also is in good agreement with experimental estimates of 3.08 and 3.14 kcal/mol.[85,86] However, there is a notable disagreement between the calculated and experimental values for the CC—OC dihedral angle in the gauche conformer. The electron diffraction data[84] suggest that this torsional angle is 84 ± 6° while the MP2/aug-cc-pVTZ optimization yields a value of 70.5°. It is likely that the electron diffraction value is in error, especially in light of infrared spectral measurements, which yield a potential energy curve with the minimum at 64°.[85] Methyl propyl ether (Fig. S2, Supplementary Material) has four conformers, *ga*, *aa*, *gg*, and *ag*, which have been studied previously at the MP2/6-31G(d)//MP2/3-21G(d) level.[114] The MP2/TZ//DZ method predicts, in agreement with previous theoretical results, that the *ga* conformer (CC—CO 60°, CC—OC –178°) is the global minimum followed by the *aa* conformer. It should be noted that the experimental structure determination of methyl propyl ether rests on the assumption that the *aa* conformer is the dominant species.[115] If the *ga* conformer is indeed the global energy minimum, reanalysis of structural data for this compound may be needed. The barrier to the internal rotation in secondary aliphatic ethers is significantly smaller than in primary ethers. The calculated barrier in isopropyl methyl ether, 1.80 kcal/mol, is in good agreement with the experimental value of 1.73 kcal/mol.[87]

Hemiacetals

Methoxymethanol is the simplest hemiacetal, and several previous studies have looked into the conformational properties of this molecule.[88,94] It is an important model for the anomeric effect (the O—C—O unit prefers a gauche orientation) and methoxymethanol has been used to parameterize force fields for carbohydrates. We find, in accord with previous results, that the g^+g^+ conformer is the global minimum for methoxymethanol (Fig. S3, Supplementary
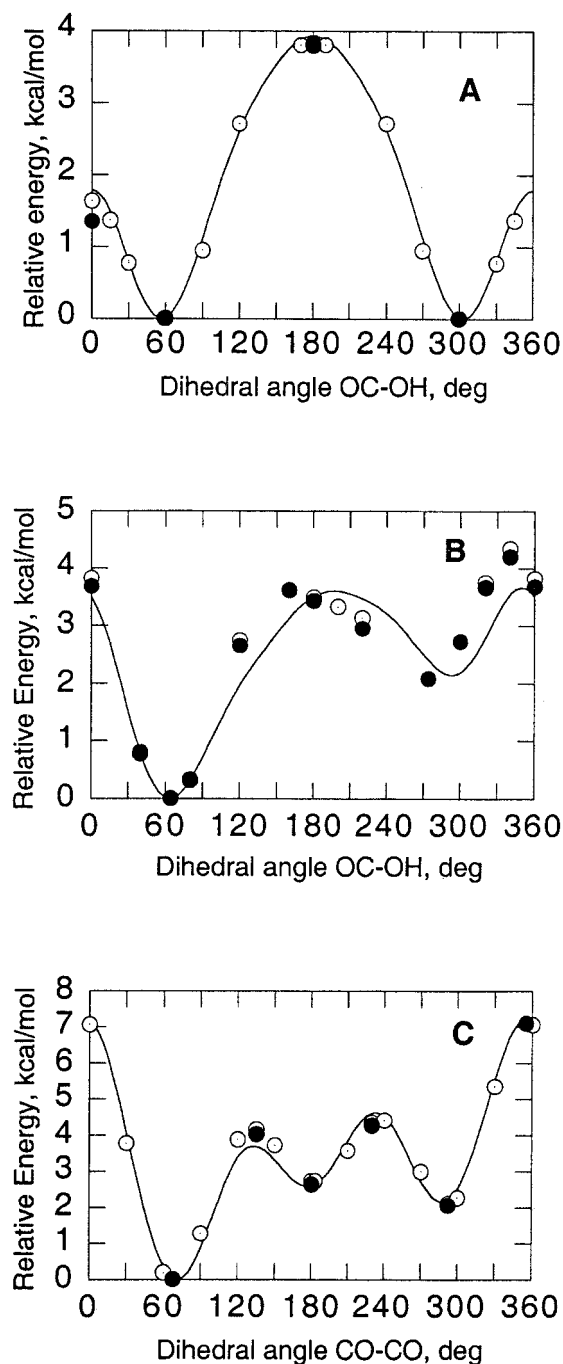

Figure 3. Torsional profiles for methoxymethanol. (A) OC—OH rotation with OC—OC anti. (B) OC—OH rotation with OC—OC gauche⁺. (C) OC—OC rotation with OC—OH gauche⁺. Open circles, MP2/aug-cc-pVDZ; closed circles, MP2/TZ//DZ; solid line, OPLS-AA.
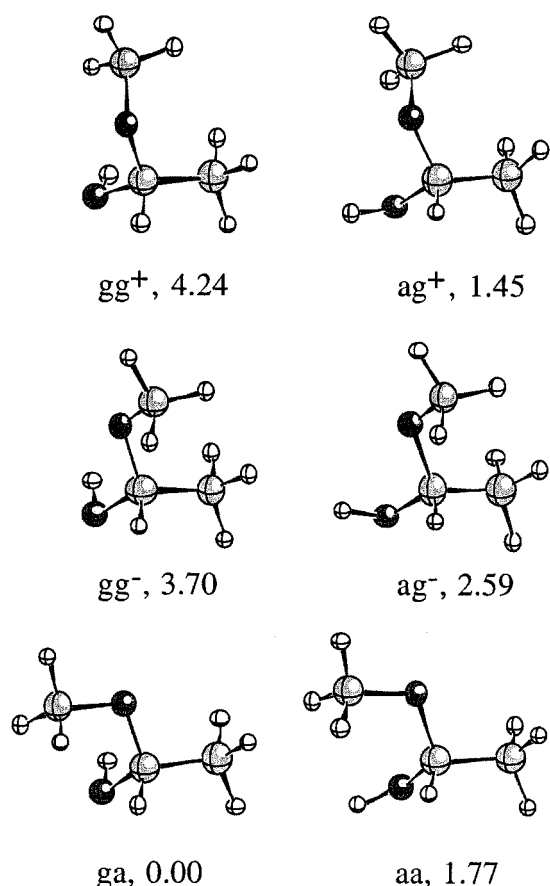
Figure 4. Conformers and their relative energies (in kcal/mol) of (*R*)-1-methoxyethanol at the MP2/TZ//DZ level.

dihedral where the fragment N(amide)—CT is part of the pipecolinyl ring. The torsional profile for this molecule is shown in Figure 6. In order to assign force field parameters for this dihedral, torsional profiles for the CT—CT—C=O and HC—CT—C=O dihedrals were also independently determined for methyl propionate and methyl acetate. Methyl propionate has been studied with the MP2 and DFT methods employing the 6-31G(d) basis set;[90] we find that MP2/TZ//DZ yields a slightly lower torsional barrier (Fig. 7) than the previously reported one. We have performed a limited number of calculations on other esters in order to verify the suitability of the MP2/TZ/DZ method. More extensive study of rotational profiles in esters has been published very recently using the HF/6-31G(d) method.[37] We find, in accord with the literature data, that the ester moiety can adopt two orientations around the $C(sp^2)$—$O(sp^3)$ bond with the Z (cis) form being more stable. Barriers for the rotation around this bond are known to be around 10–15 kcal/mol from the Z conformer.[89,90] Our MP2 energy difference between Z and E conformers of methyl formate (5.45 kcal/mol) is larger than the experimental value, 4.75 ± 0.19, but the energy difference for methyl acetate (7.47 kcal/mol) is in the lower end of the experimental value, 8.5 ± 1.0.[89] The structure of methyl acetate at the MP2/aug-cc-pVTZ level is very similar to the experimental geometry from joint electron diffraction-microwave-infrared analysis.[116]
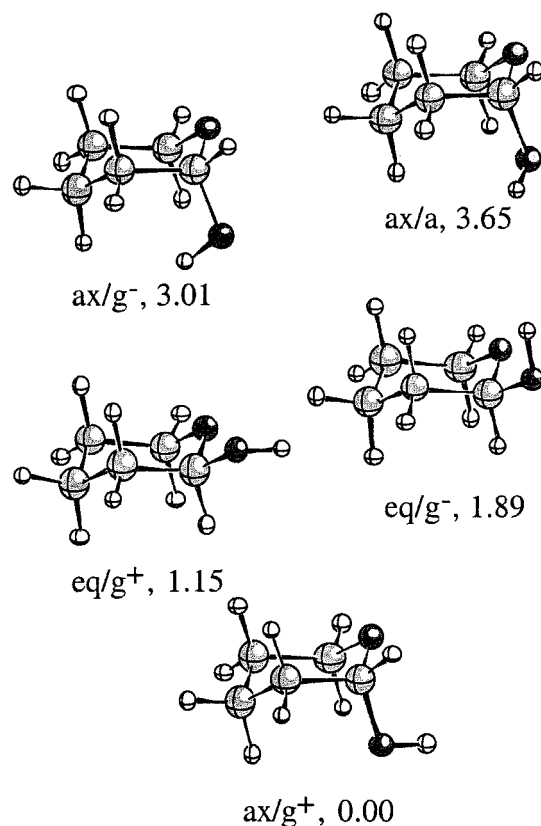
Material). The two other minima at the MP2/TZ//DZ potential energy surface are $g^- g^+$ (2.05 kcal/mol) and ag^+ (2.64 kcal/mol). Interestingly, the *aa* form (6.43 kcal/mol) was found to be a transition state at this level of theory instead of a high energy minimum as was previously thought.[88] The *ga* structure was not a local minimum at the MP2/aug-cc-pVDZ level (Fig. 3B), in accord with previous MP2/6-31+G(d) results.[88] Figure 3 displays energy profiles for the rotation around the HO—CO and CO—CO bonds in methoxymethanol. It was also found that the rotation of the methyl group around the O—CH$_3$ bond in hemiacetals faces a significantly lower energy barrier than a similar rotation in ethers (Table 1). Six stable conformers were located for methoxyethanol (Fig. 4) and five energy minima were found on the energy surface of tetrahydropyran-2-ol (Fig. 5). The anti orientation of the hydroxyl group in equatorial tetrahydropyran-2-ol was a transition state at the MP2/aug-cc-pVDZ level. Interestingly, the structure with the H—O—C—O dihedral at 171° and an axial hydroxyl group was a local minimum.

Esters

The study of the ester moiety was inspired by the need to know the torsional barrier in pipecolinyl esters, which is a part of the polyketide structure. This molecule presents a unique N(amide)—CT—C=O

Figure 5. Conformers and their relative energies (in kcal/mol) of tetrahydropyran-2-ol at the MP2/aug-cc-pVDZ level. For visual comparison, axial conformers are shown in the *S* configuration and equatorial conformers are shown in the *R* configuration.
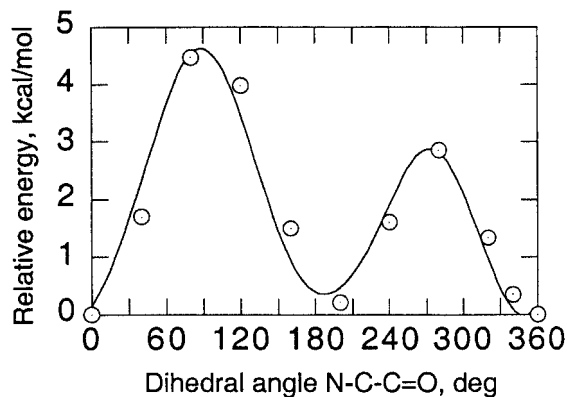
Figure 6. Torsional profile for the NC—CO rotation in the pipecolinyl ester. Open circles, MP2/6-31+G(d,p); solid line, OPLS-AA.

The barrier for the C—CH$_3$ rotation in ethyl acetate was found to be 0.19 kcal/mol; this can be compared to the experimental value of 0.29 kcal/mol.[61] The barrier for the rotation around the O—CH$_3$ bond depends on the conformation around the C(sp^2) —O(sp^3) bond.[60] This barrier is about 1.2 kcal/mol in Z forms of methyl esters while negligible barrier is present in E-conformers. The MP2 calculations reproduce these features very well and it appears that the MP2/TZ//DZ method is reliable in calculating the conformational energies of esters.

Glyoxal Analogs

Ab initio studies on glyoxal analogs have been published recently.[63] We have extended these studies to five additional analogs, which, along with the data on alcohols, hemiacetals, and ethers, allowed derivation of torsional parameters for the pyranosyl moiety of polyketides. Seven conformations were found for 3-hydroxy-2-oxopropanal (pyruvaldehyde) at the MP2/aug-cc-pVDZ level. The lowest energy conformer (Fig. 8) showed C$_s$ symmetry and an intramolecular hydrogen bond between the hydroxyl hydrogen and an adjacent carbonyl group. In the second conformer,
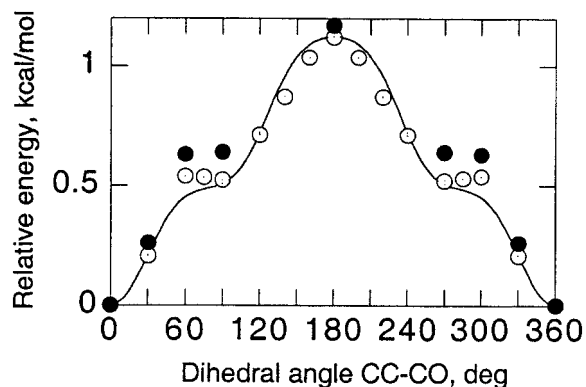

Figure 7. Torsional profile for the CC—CO rotation in methyl propionate. Open circles, MP2/aug-cc-pVDZ; closed circles, MP2/TZ//DZ; solid line, OPLS-AA.

tg$^+$g$^-$, 4.79   cea, 9.45

tea, 4.17   cta, 7.79
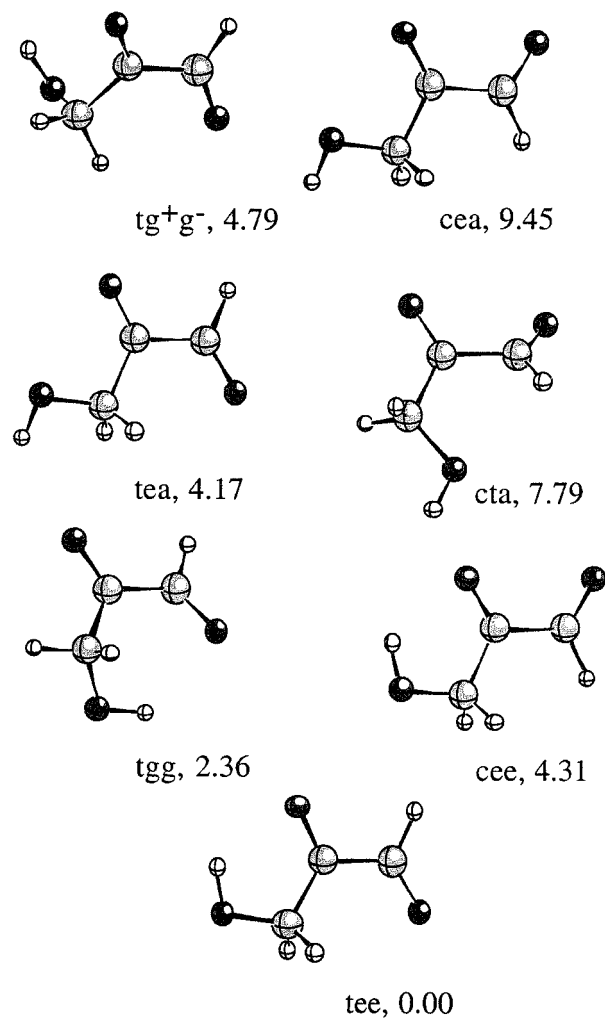
tgg, 2.36   cee, 4.31

tee, 0.00

Figure 8. Conformers and their relative energies (in kcal/mol) of 3-hydroxy-2-oxopropanal at the MP2/DZ//TZ level.

the intramolecular hydrogen bond was to a distal carbonyl group. The analogous molecule, 3-methoxy-2-oxopropanal, had eight stable conformers (Fig. 9), but because of the lack of intramolecular hydrogen bonding, the relative energy ordering is quite different than in the hydroxyl analog. The torsional profiles for 3-hydroxy-2-oxopropanal and 3-methoxy-2-oxopropanal are shown in Figure 10 and Figure 11, respectively. Four low-energy conformers were found for 3-hydroxy-3-methoxy-2-oxopropanal (Fig. S4, Supplementary Material) and for 2-glyoxoyl-tetrahydropyran (Fig. S5, Supplementary Material), and six minima were located for 2-glyoxoyl-tetrahydropyran-2-ol (Fig. S6, Supplementary Material). It is likely that additional high-energy minima for these molecules exist. It is noteworthy that in 3-hydroxy-3-methoxy-2-oxopropanal and 2-glyoxoyl-tetrahydropyran-2-ol the structure with a hydrogen bond between the hydroxyl group and distal carbonyl is a global minimum, contrary to the order of stabilities in 3-hydroxy-2-oxopropanal. This effect cannot be reproduced accurately with the original nor present OPLS–AA parameterization and appears to be a deficiency in treatment of nonbonded interactions.
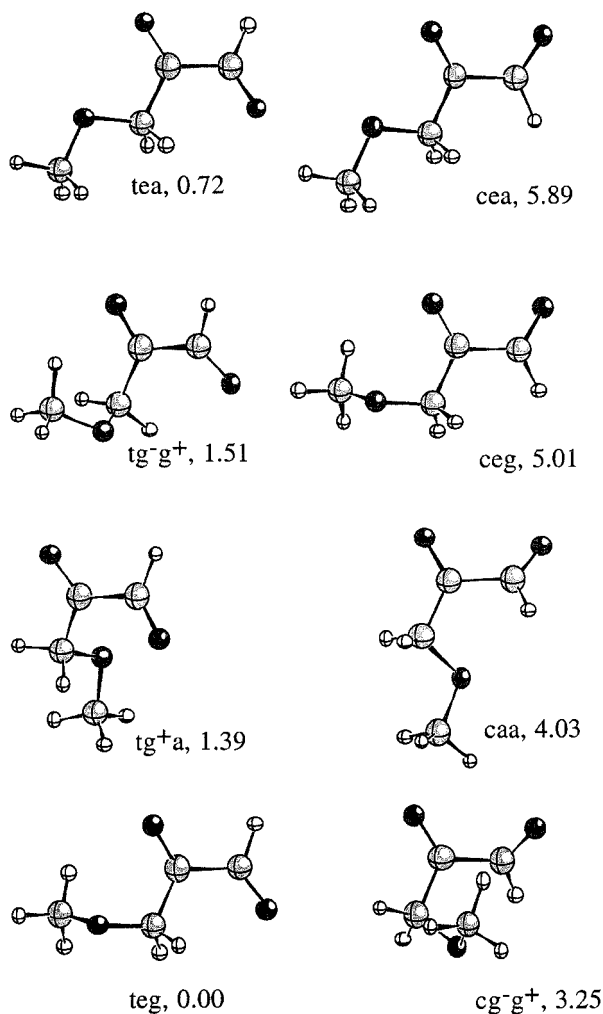
Figure 9. Conformers and their relative energies (in kcal/mol) of 3-methoxy-2-oxopropanal at the MP2/DZ//TZ level.

Accuracy of the Force Field

Recent comparison of the several common force fields has shown that conformational energies are often predicted with RMS deviations in excess of 1 kcal/mol from experimental or accurate *ab initio* data.[32] It has also been demonstrated that accuracy of predictions can be increased significantly by careful parameterization of force constants based on *ab initio* data and RESP charges.[117] Comparison of present OPLS–AA and MP2 conformational energies from Tables 1 and 5 shows that, when supplied with proper torsional parameters, the OPLS–AA force field can accurately reproduce conformational energies of organic molecules containing sp³ carbons and oxygens in various molecular environments. Significant improvement over the standard OPLS–AA parameters is seen with alcohols, ethers, and hemiacetals. For alcohols (see Supplementary Material) the maximum error is reduced from 2.03 kcal/mol to 0.93 kcal/mol, and RMS deviation has decreased from 0.56 kcal/mol to 0.34 kcal/mol. The maximum deviation among all molecules, 1.42 kcal/mol, is found for the energy difference be-

tween the twist-boat and chair conformers of oxane. Overall RMS deviation of OPLS–AA data from the reference (either MP2/TZ//DZ or previously published data) conformational energies and torsional barrier heights is 0.39 kcal/mol for alkanes, alcohols,
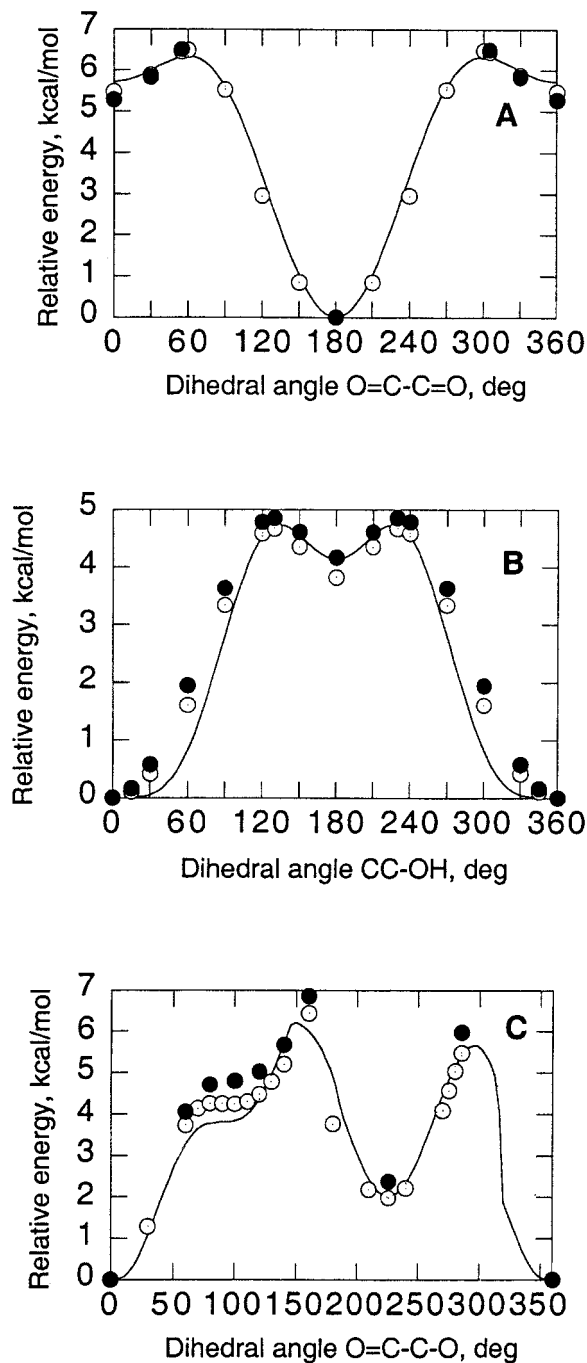

Figure 10. Torsional profiles for 3-hydroxy-2-oxopropanal. (A) O=C—C=O rotation with CC—OH anti. (B) CC—OH rotation with O=C—C=O *s*-trans. (C) O=C—C—O rotation with O=C—C=O *s*-trans. Open circles, MP2/aug-cc-pVDZ; closed circles, MP2/TZ//DZ; solid line, OPLS-AA.
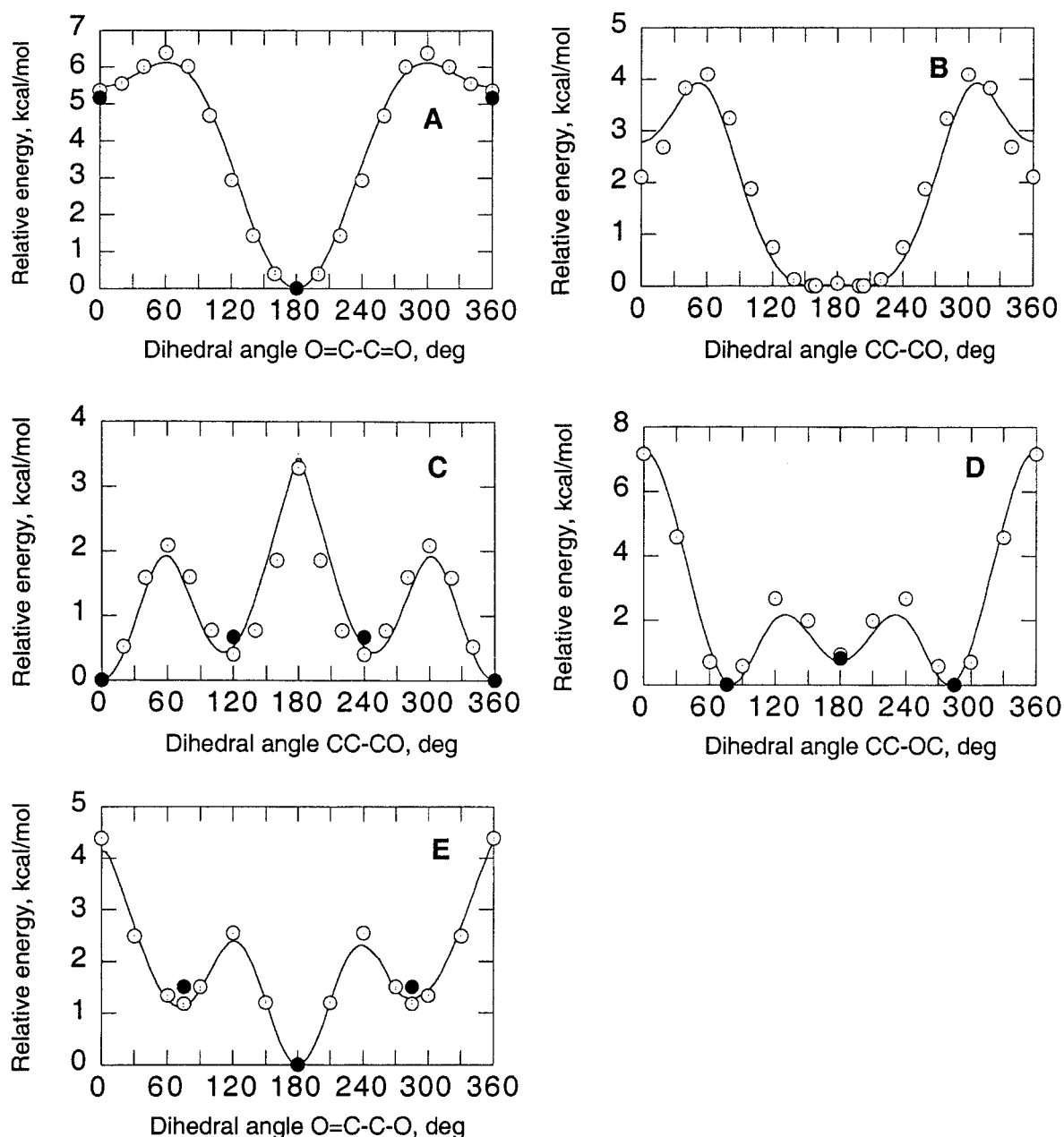
Figure 11. Torsional profiles for 3-methoxy-2-oxopropanal. (A) O═C—C═O rotation with CC—OC anti. (B) CC—CO rotation with O═C—C═O *s*-cis. (C) CC—CO rotation with O═C—C═O *s*-trans. (D) CC—OC rotation with O═C—C═O *s*-trans. (E) O═C—C—O rotation with O═C—C═O *s*-trans and O—CH₃ gauche. Open circles, MP2/aug-cc-pVDZ; closed circles, MP2/TZ//DZ; solid line, OPLS-AA.

ethers, and hemiacetals (Table 5). Thus, current parameters give conformational energies with qualities similar to the MMFF[32] and recently reparameterized RESP-based AMBER.[117] It should be pointed out that Jorgensen has very recently proposed a new set of alkane torsional parameters, which appear to be of comparable quality to parameters reported here.[37]

Statistical analysis of bulk properties of alkanes, alcohols, and ethers with current parameters shows that molar volumes of liquids from simulations are on average within 1.1% of the corresponding

experimental values. The largest error, 2.9%, occurs with neopentane. We note that the experimental molar volume of neopentane at 9.5°C has not been directly measured but was obtained by extrapolating the experimental density data. The mean error for heats of vaporization of 19 compounds from Table 4 is 2.4%. Notable deviations from experimental data occur with neopentane and diethyl ether. Overall, current parameters perform slightly better than the original OPLS–AA parameterization at the expense of additional nonbonded parameters for secondary and tertiary

carbons. This allows, among other things, a correct prediction of the relative densities and heats of vaporization of 1-propanol and 2-propanol.

Tetraketides as Potent Neuroregenerative Agents

Our main finding pertaining to the design of neuroregenerative drugs is that tetraketides with minimally modified linker regions are predicted to adopt low-energy conformations that are similar to the drug FK506 bound to protein FKBP12. Thus, they are likely to bind tightly to protein FKBP52 as well, and may possess neuro-regenerative activity. It has been demonstrated previously that the linker region of tetraketide is too small for efficient binding of calcineurin; in other words, tetraketides are predicted to be non-immunosuppressive.[118] Conformational analysis has been used in the past to identify tetraketides with favorable binding properties using MM3(94) force field.[19] By comparing the structures obtained with this method to current conformers, we note that the torsion around the N—C—C≡O bond in pipecolinyl esters is described very differently by the two force fields. Based on *ab initio* calculations, OPLS–AA predicts potential energy minima near zero and 180° while MM3 yields energy minimum at around 90°. This behavior was also found in the pipecolinyl ester model MPIP, for which MM3 predicted a minimum with N—C—C≡O dihedral at −73°. This discrepancy arises most likely from the fact that the N—C—C≡O dihedral in the MM3 is parameterized based on peptides. This torsional parameter is apparently not transferable from peptides to pipecolinyl esters and thus MM3 force field does not describe this portion of polyketides accurately. Conversely, the current polyketide N—C—C≡O torsional parameter should not be used for peptides.
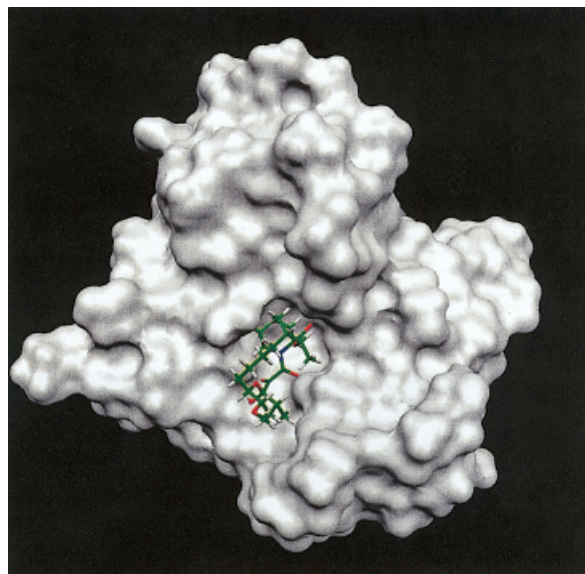

Figure 12. The lowest energy conformation of a tetraketide C (Chart 3) docked to the binding site of the rabbit FKBP52 protein. The pipecolinyl ring and ketoamide moiety lie at the bottom of the cavity with the linker region protruding from the protein. The image was produced with the program MOLEKEL.[105]

Table 5. Summary Comparison of *Ab Initio* and OPLS-AA Conformational Energies.

Class	MP2/DZ vs. MP2/TZ//DZ			OPLS-AA vs. Target[a]		
	Max[b]	RMSD	No	Max	RMSD	No
Alkanes	0.22	0.10	11	0.93	0.42	19
Alcohols	0.29	0.16	36	0.99	0.34	36
Ethers	0.29	0.11	15	1.42	0.42	19
Hemiacetals	0.18	0.09	12	1.39	0.46	17
Esters	0.20	0.11	14	1.17	0.56	17
Glyoxals	0.55	0.27	17	1.87	0.75	17
Overall	0.55	0.16	106	1.87	0.48	126

[a]The MP2/TZ//DZ data, when available, were used for target values. When the MP2/TZ//DZ data were not available, previously published reliable experimental or *ab initio* data from Table 1 were used. For tetrahydropyran-2-ol, MP2/aug-cc-pVDZ relative energies were used.
[b]Abbreviations used: Max—maximum absolute difference of conformational energies (kcal/mol); RMSD—root mean square deviation (kcal/mol); No—number of relative energies values that were included in the comparison.

Conclusions

High-level *ab initio* structures, conformational energies, and torsional energy profiles, along with Monte Carlo liquid simulations, have been used to derive new parameters for the OPLS–AA force field. The resulting force field yields reliable information on the shape of potential energy surfaces for alcohols, ethers, esters, hemiacetals, and glyoxal derivatives. Conformational analysis of polyketides using this force field suggests that tetraketides containing a simple aliphatic effector domain would bind the target protein FKBP with an affinity similar to FK506 while not interacting with calcineurin. These properties, along with the possibility of synthesis of tetraketides via engineered biosynthesis, make tetraketides attractive neuroregenerative agents that lack the immunosuppressive side effect.

Note Added in Proof

Very recent high level *ab initio* study of pentane revealed that the *ag* and *gg* conformers are 0.62 and 1.06 kcal/mol above the *aa* global minimum (Salam, A.; Deleuze, M. S. J Chem Phys 2002, 116, 1296). When these data are used as target values, RMDS for alkanes (Table 5) decreases from 0.42 to 0.39 kcal/mol.

Acknowledgments

initial structures of methoxymethanol and tetrahydropyran-2-ol in computer-readable format, Dr. William L. Jorgensen for making the manuscript of their work[37] available before publication, and Dr. Helgi Adalsteinsson for helpful discussions that concerned the conformational analysis of polyketides.

Supplementary Material

Six additional figures showing the conformers of some of the molecules and a table comparing the performance of current parameters with the standard OPLS–AA force field are included in the Supplementary Material. Cartesian coordinates of all stable conformers for molecules discussed in this work are provided. Interested readers can obtain the structures of torsional saddle points and of nonstationary points by contacting the authors.

References

1. Birch, A. J. Science 1967, 156, 202.
2. Katz, L. Chem Rev 1997, 97, 2557.
3. Khosla, C. Chem Rev 1997, 97, 2577.
4. Paterson, I.; Scott, J. P. Tetrahedron Lett 1997, 38, 7445.
5. Gold, B. G. Drug Metab Rev 1999, 31, 649.
6. Gold, B. G. Expert Opin Investig Drugs 2000, 9, 2331.
7. Gold, B. G.; Densmore, V.; Shou, W.; Matzuk, M. M.; Gordon, H. S. J Pharmacol Exp Ther 1999, 289, 1202.
8. Hamilton, G. S.; Steiner, J. P. J Med Chem 1998, 41, 5119.
9. Harding, M. W.; Galat, A.; Uehling, D. E.; Schreiber, S. L. Nature 1989, 341, 758.
10. Griffith, J. P.; Kim, J. L.; Kim, E. E.; Sintchak, M. D.; Thomson, J. A.; Fitzgibbon, M. J.; Fleming, M. A.; Caron, P. R.; Hsiao, K.; Navia, M. A. Cell 1995, 82, 507.
11. Babine, R. E.; Bender, S. L. Chem Rev 1997, 97, 1359.
12. Van Duyne, G. D.; Standaert, R. F.; Karplus, P. A.; Schreiber, S. L.; Clardy, J. Science 1991, 252, 839.
13. Steiner, J. P.; Hamilton, G. S.; Ross, D. T.; Valentine, H. L.; Guo, H.; Connolly, M. A.; Liang, S.; Ramsey, C.; Li, J.-H. J.; Huang, W.; Howorth, P.; Soni, R.; Fuller, M.; Sauer, H.; Nowotnik, A. C.; Suzdak, P. D. Proc Natl Acad Sci USA 1997, 94, 2019.
14. Gold, B. G. Mol Neurobiol 1997, 15, 285.
15. Gold, B. G.; Zeleny-Pooley, M.; Wang, M. S.; Chaturvedi, P.; Armistead, D. M. Exp Neurol 1997, 147, 269.
16. Schreiber, S. L. Science 1991, 251, 283.
17. Pratt, W. B.; Toft, D. O. Endocr Rev 1997, 18, 306.
18. Craescu, C. T.; Rouvière, N.; Popescu, A.; Cerpolini, E.; Lebeau, M.-C.; Baulieu, E. E.; Mispelter, J. Biochemistry 1996, 35, 11045.
19. Adalsteinsson, H.; Bruice, T. C. Bioorg Med Chem 2000, 8, 625.
20. Weiner, S. J.; Kollman, P. A.; Case, D. A.; Singh, U. C.; Ghio, C.; Alagona, G.; Profeta, S., Jr.; Weiner, P. J Am Chem Soc 1984, 106, 765.
21. Cornell, W. D.; Cieplak, P.; Bayly, C. I.; Gould, I. R.; Merz, K. M., Jr.; Ferguson, D. M.; Spellmeyer, D. C.; Fox, T.; Caldwell, J. W.; Kollman, P. A. J Am Chem Soc 1995, 117, 5179.
22. Rasmussen, K.; Engelsen, S. B. In The Consistent Force Field: Development of potential energy functions for conformational analysis; Recent Experimental and Computational Advances in Molecular Spectroscopy, Vol. 406; Fausto, R., Ed.; Kluwer Academic Publishers: Dordrecht, 1993, p. 381.
23. Ewig, C. S.; Thacher, T. S.; Hagler, A. T. J Phys Chem B 1999, 103, 6998.
24. Brooks, B. R.; Bruccoleri, R. E.; Olafson, B. D.; States, D. J.; Swaminathan, S.; Karplus, M. J Comput Chem 1983, 4, 187.
25. MacKerell, A. D., Jr.; Bashford, D.; Bellott, M.; Dunbrack, R. L.; Evanseck, J. D.; Field, M. J.; Fischer, S.; Gao, J.; Guo, H.; Ha, S.; Joseph-McCarthy, D.; Kuchnir, L.; Kuczera, K.; Lau, F. T. K.; Mattos, C.; Michnick, S.; Ngo, T.; Nguyen, D. T.; Prodhom, B.; Reiher, W. E.; Roux, B.; Schlenkrich, M.; Smith, J. C.; Stote, R.; Straub, J.; Watanabe, M.; Wiórkiewicz-Kuczera, J.; Yin, D.; Karplus, M. J Phys Chem B 1998, 102, 3586.
26. Sun, H. J Phys Chem B 1998, 102, 7338.
27. Scott, W. R. P.; Hünenberger, P. H.; Tironi, I. G.; Mark, A. E.; Billeter, S. R.; Fennen, J.; Torda, A. E.; Huber, T.; Krüger, P.; van Gunsteren, W. F. J Phys Chem A 1999, 103, 3596.
28. Derreumaux, P.; Vergoten, G. J Chem Phys 1995, 102, 8586.
29. Allinger, N. L.; Yuh, Y. H.; Lii, J.-H. J Am Chem Soc 1989, 111, 8551.
30. Allinger, N. L.; Chen, K. S.; Lii, J. H. J Comput Chem 1996, 17, 642.
31. Jorgensen, W. L.; Maxwell, D. S.; Tirado-Rives, J. J Am Chem Soc 1996, 118, 11225.
32. Halgren, T. A. J Comput Chem 1999, 20, 730.
33. Halgren, T. A. J Comput Chem 1996, 17, 490.
34. Kaminski, G.; Jorgensen, W. L. J Phys Chem 1996, 100, 18010.
35. McDonald, N. A.; Jorgensen, W. L. J Phys Chem B 1998, 102, 8049.
36. Rizzo, R. C.; Jorgensen, W. L. J Am Chem Soc 1999, 121, 4827.
37. Price, M. L.; Ostrovsky, D.; Jorgensen, W. L. J Comput Chem 2001, 22, 1340.
38. Jorgensen, W. L.; McDonald, N. A. J Mol Struct (THEOCHEM) 1998, 424, 145.
39. Damm, W.; Frontera, A.; Tirado-Rives, J.; Jorgensen, W. L. J Comput Chem 1997, 18, 1955.
40. Watkins, E. K.; Jorgensen, W. L. J Phys Chem A 2001, 105, 4118.
41. Kaminski, G. A.; Friesner, R. A.; Tirado-Rives, J.; Jorgensen, W. L. J Phys Chem B 2001, 105, 6474.
42. Allinger, N. L.; Fermann, J. T.; Allen, W. D.; Schaefer, H. F. J Chem Phys 1997, 106, 5143.
43. Tozer, D. J. Chem Phys Lett 1999, 308, 160.
44. Frisch, M. J.; Trucks, G. W.; Schlegel, H. B.; Scuseria, G. E.; Robb, M. A.; Cheeseman, J. R.; Zakrzewski, V. G.; Montgomery, J. A. J.; Stratmann, R. E.; Burant, J. C.; Dapprich, S.; Millam, J. M.; Daniels, A. D.; Kudin, K. N.; Strain, M. C.; Farkas, O.; Tomasi, J.; Barone, V.; Cossi, M.; Cammi, R.; Mennucci, B.; Pomelli, C.; Adamo, C.; Clifford, S.; Ochterski, J.; Petersson, G. A.; Ayala, P. Y.; Cui, Q.; Morokuma, K.; Malick, D. K.; Rabuck, A. D.; Raghavachari, K.; Foresman, J. B.; Cioslowski, J.; Ortiz, J. V.; Stefanov, B. B.; Liu, G.; Liashenko, A.; Piskorz, P.; Komaromi, I.; Gomperts, R.; Martin, R. L.; Fox, D. J.; Keith, T.; Al-Laham, M. A.; Peng, C. Y.; Nanayakkara, A.; Gonzalez, C.; Challacombe, M.; Gill, P. M. W.; Johnson, B.; Chen, W.; Wong, M. W.; Andres, J. L.; Gonzalez, C.; Head-Gordon, M.; Replogle, E. S.; Pople, J. A. Gaussian 98; Gaussian, Inc.: Pittsburgh, PA, 1998.
45. He, Y.; Cremer, D. J Phys Chem A 2000, 104, 7679.
46. Helgaker, T.; Gauss, J.; Jørgensen, P.; Olsen, J. J Chem Phys 1997, 106, 6430.
47. Jorgensen, W. L. BOSS Version 4.2; Yale University: New Haven, CT, 2000.
48. Singh, U. C.; Kollman, P. A. J Comput Chem 1984, 5, 129.
49. Bayly, C. I.; Cieplak, P.; Cornell, W. D.; Kollman, P. A. J Phys Chem 1993, 97, 10269.
50. Hirota, E.; Saito, S.; Endo, Y. J Chem Phys 1979, 71, 1183.
51. Goodman, L.; Pophristic, V.; Weinhold, F. Acc Chem Res 1999, 32, 983.

52. Dixon, D. A.; Komornicki, A. J Phys Chem 1990, 94, 5630.
53. Rocha, W. R.; Pliego, J. R.; Resende, S. M.; Dos Santos, H. F.; De Oliveira, M. A.; De Almeida, W. B. J Comput Chem 1998, 19, 524.
54. Wiberg, K. B.; Hammer, J. D.; Castejon, H.; Bailey, W. F.; DeLeon, E. L.; Jarret, R. M. J Org Chem 1999, 64, 2085.
55. Pophristic, V.; Goodman, L. J Phys Chem A 2000, 104, 3231.
56. Tsuzuki, S.; Uchimaru, T.; Tanabe, K. J Mol Struct (THEOCHEM) 1996, 366, 89.
57. Freeman, F.; Kasner, J. A.; Kasner, M. L.; Hehre, W. J. J Mol Struct (THEOCHEM) 2000, 496, 19.
58. Smith, B. J. J Phys Chem A 1998, 102, 3756.
59. Williams, D. J.; Hall, K. B. J Phys Chem 1996, 100, 8224.
60. Wiberg, K. B.; Bohn, R. K.; Jimenez-Vazquez, H. J Mol Struct 1999, 485–486, 239.
61. Sheridan, J.; Bossert, W.; Bauder, A. J Mol Spectrosc 1980, 80, 1.
62. Bohn, R. K.; Wiberg, K. B. Theor Chem Acc 1999, 102, 272.
63. Kahn, K.; Bruice, T. C. Bioorg Med Chem 2000, 8, 1881.
64. Hoyland, J. R. J Chem Phys 1968, 49, 1908.
65. Herrebout, W. A.; van der Veken, B. J.; Wang, A.; Durig, J. R. J Phys Chem 1995, 99, 578.
66. Lide, D. R. J.; Mann, D. E. J Chem Phys 1958, 29, 914.
67. Kanesaka, I.; Snyder, R. G.; Strauss, H. L. J Chem Phys 1986, 84, 395.
68. Wiberg, K. B.; Murcko, M. A. J Am Chem Soc 1988, 110, 8029.
69. Verma, A. L.; Murphy, W. F.; Bernstein, H. J. J Chem Phys 1974, 60, 1540.
70. Weiss, S.; Leroi, G. E. Spectrochim Acta A 1969, 25, 1759.
71. Snyder, R. G.; Schachtschneider, J. H. Spectrochim Acta 1965, 21, 169.
72. Whalon, M. R.; Bushweller, C. H.; Anderson, W. G. J Org Chem 1984, 49, 1185.
73. De Lucia, F. C.; Herbst, E.; Anderson, T.; Helminger, P. J Mol Spectrosc 1989, 134, 395.
74. Xu, L. H.; Lees, R. M.; Hougen, J. T. J Chem Phys 1999, 110, 3835.
75. Durig, J. R.; Larsen, R. A. J Mol Struct 1989, 238, 195.
76. Senent, M. L.; Smeyers, Y. G.; Dominguez-Gómez, R.; Villa, M. J Chem Phys 2000, 112, 5809.
77. Dreizler, H.; Scappini, F. Z Naturforsch 1981, 36A, 1187.
78. Hirota, E. J Phys Chem 1979, 83, 1457.
79. Suwa, A.; Ohta, H. J Mol Struct 1988, 172, 275.
80. Xu, S.; Liu, Y.; Sha, G.; Zhang, C.; Xie, J. J Phys Chem A 2000, 104, 8671.
81. Wang, F.; Polavarapu, P. L. J Phys Chem A 2000, 104, 10683.
82. Groner, P.; Durig, J. R. J Chem Phys 1977, 66, 1856.
83. Durig, J. R.; Li, Y. S.; Groner, P. J Mol Spectrosc 1976, 62, 159.
84. Oyanagi, K.; Kuchitsu, K. Bull Chem Soc Jpn 1978, 51, 2237.
85. Durig, J. R.; Compton, D. A. C. J Chem Phys 1978, 69, 4713.
86. Perchard, J. P. J Mol Struct 1970, 6, 457.
87. Nakagawa, J.; Imachi, M.; Hayashi, M. J Mol Struct 1984, 112, 201.
88. Ganguly, B.; Fuchs, B. J Org Chem 1997, 62, 8892.
89. Blom, C. E.; Günthard, H. H. Chem Phys Lett 1981, 84, 267.
90. Blomqvist, J.; Ahjopalo, L.; Mannfors, B.; Pietilä, L.-O. J Mol Struct (THEOCHEM) 1999, 488, 247.
91. Tanaka, Y. Acustica 1970, 23, 328.
92. Riveros, J. M.; Wilson, E. B., Jr. J Chem Phys 1967, 46, 4605.
93. George, W. O.; Hassid, D. V.; Maddams, W. F. J Chem Soc, Perkin Trans 2 1972, 1798.
94. Halgren, T. A.; Nachbar, R. B. J Comput Chem 1996, 17, 587.
95. Michl, J.; West, R. Acc Chem Res 2000, 33, 821.
96. Haraschta, P.; Heintz, A.; Lehmann, J. K.; Peters, A. J Chem Eng Data 1999, 44, 932.
97. Haynes, W. M. J Chem Eng Data 1983, 28, 367.
98. McLure, I. A.; Barbarin-Castillo, J. M. Int J Thermophys 1993, 14, 1173.
99. Brocos, P.; Calvo, E.; Bravo, R.; Pintos, M.; Amigo, A.; Roux, A. H.; Roux-Desgranges, G. J Chem Eng Data 1999, 44, 67.
100. Obama, M.; Oodera, Y.; Kohama, N.; Yanase, T.; Saito, Y.; Kusano, K. J Chem Eng Data 1985, 30, 1.
101. Maass, O.; Boomer, E. H. J Am Chem Soc 1922, 44, 1709.
102. Kennedy, R. M.; Sagenkahn, M.; Aston, J. G. J Am Chem Soc 1941, 63, 2267.
103. Afeefy, H. Y.; Liebman, J. F.; Stein, S. E. Neutral Thermochemical Data; Mallard, W. G., Linstrom, P. J., Ed.; National Institute of Standards and Technology: Gaithersburg, MD, 2000, (http://webbook.nist.gov).
104. Motamedi, H.; Shafiee, A. Eur J Biochem 1998, 256, 528.
105. Portmann, S.; Lüthi, H. P. CHIMIA 2000, 54, 766.
106. Egawa, T.; Moriyama, H.; Takeuchi, H.; Konaka, S.; Siam, K.; Schäfer, L. J Mol Struct 1993, 298, 37.
107. Takeuchi, H.; Sugino, M.; Egawa, T.; Konaka, S. J Phys Chem 1993, 97, 7511.
108. Coussan, S.; Bouteiller, Y.; Perchard, J. P.; Zheng, W. Q. J Phys Chem A 1998, 102, 5789.
109. Lide, D. R. J Chem Phys 1960, 33, 1514.
110. Iijima, T. J Mol Struct 1989, 212, 137.
111. Florián, J.; Leszczynski, J.; Johnson, B. G.; Goodman, L. Mol Physics 1997, 91, 439.
112. Adya, A. K.; Bianchi, L.; Wormald, C. J. J Chem Phys 2000, 112, 4231.
113. Schaal, H.; Häber, T.; Suhm, M. A. J Phys Chem A 2000, 104, 265.
114. Gil, F. P. S. C.; Teixeira-Dias, J. J. C. J Mol Struct (THEOCHEM) 1996, 363, 311.
115. Kato, H.; Nakagawa, J.; Hayashi, M. J Mol Spectrosc 1980, 80, 272.
116. Pyckhout, W.; Van Alsenoy, C.; Geise, H. J. J Mol Struct 1986, 144, 265.
117. Wang, J.; Cieplak, P.; Kollman, P. A. J Comp Chem 2000, 21, 1049.
118. Adalsteinsson, H.; Bruice, T. C. Bioorg Med Chem 2000, 8, 617.